

SU-4240-613
 hep-ph/9506473
 June, 1995

Effects of Symmetry Breaking on the Strong and Electroweak Interactions of the Vector Nonet

Masayasu HARADA* and Joseph SCHECHTER†

Department of Physics, Syracuse University, Syracuse, NY 13244-1130, USA

Abstract

Starting from a chiral invariant and quark line rule conserving Lagrangian of pseudoscalar and vector nonets we introduce first and second order symmetry breaking as well as quark line rule violating terms and fit the parameters, at tree level, to many strong and electroweak processes. A number of predictions are made. The electroweak interactions are included in a manifestly gauge invariant manner. The resulting symmetry breaking pattern is discussed in detail. Specifically, for the “strong” interactions, we study all the vector meson masses and $V \rightarrow \phi\phi$ decays, including isotopic spin violations. In the electroweak sector we study the $\{\rho^0, \omega, \phi\} \rightarrow e^+e^-$ decays, $\{\pi^+, K^+, K^0\}$ “charge radii”, K_{l3} “slope factor” and the overall $e^+e^- \rightarrow \pi^+\pi^-$ process. It is hoped that the resulting model may be useful as a reasonable description of low energy physics in the range up to about 1 GeV.

* e-mail address : mharada@npac.syr.edu

† e-mail address : schechter@suhep.phy.syr.edu

1 Introduction

It seems likely that, whether or not it can be fully derived from first principles, an effective chiral Lagrangian will remain as a preferred description of low energy hadronic physics. At very low energies, near to the $\pi\pi$ threshold, the Lagrangian can be constructed in terms of only the pseudoscalar chiral fields. According to the chiral perturbation scheme[1, 2] it is possible to make a controlled energy expansion in which one first keeps terms with two derivatives or one power of the chiral symmetry breaking quark mass. This is the traditional chiral Lagrangian[3] and is to be evaluated at tree level. At the next stage of approximation, single loops are computed and their divergences are cancelled by the addition of counterterms with four derivatives or their equivalent. Each counterterm can also make a finite contribution so there are many arbitrary constants. In practice it is unrealistic to go beyond four derivative order and furthermore the finite parts of the counterterms can be largely explained[4] as contributions involving vector meson terms acting at tree level.

If one wants to extend the effective Lagrangian to describe hadronic physics up to about the 1 GeV region, it is clearly necessary to include the additional particles – the vector mesons – whose masses lie in this range. For such Lagrangians there does not seem to be an unambiguous controlled energy expansion. We might imagine keeping the energy expansion around $\pi\pi$ threshold for soft interaction of the pseudoscalars. Then, thinking of the vectors as “heavy” particles, we may make an expansion around the vector meson mass shell of the soft (chiral) interactions of the vectors. Each of these two expansions will have a limited range of validity but it may be possible to “analytically continue” between the two. This could conceivably be extended to the entire particle spectrum.

A different way to organize the low energy Lagrangian is based on the $1/N_c$ approximation to QCD[5]. In this approach *all* $\bar{q}q$ mesons should be included at *tree level* at the initial stage of approximation. The next level would contain all one loop corrections and so on. In dealing with a limited energy range it seems reasonable[6] to truncate the spectrum.

Regardless of whichever way is adopted for organizing the Lagrangian it is necessary to study the effects of tree level symmetry breaking for the vector meson nonet. This is the main goal of the present paper. It is, of course, an old subject. Very recent treatments include refs. [7, 8, 9, 10]; our treatment will follow most closely the approach and notation of the first of these. There are several new features. We shall discuss all of the vector meson masses and three point $V\phi\phi$ coupling constants (including isospin violation effects) as well as many of the electroweak observables which are related to vector meson dominance. Our

enumeration of the tree level symmetry breaking terms will be more complete than before and we shall include explicit discussion of the relatively small Okubo-Zweig-Iizuka (OZI) rule[11] violating effects for the vectors as well as “second order” terms which may be needed to fit the experimental data. We will aim for a more accurate and comprehensive fitting of the observable quantities. This will lead us to include a number of additional diagrams for various processes which are required by chiral invariance but contribute at about the 10% level and are usually neglected. (An example is the *direct* $\omega \rightarrow 2\pi$ isospin violating vertex.) In trying to fit the experimental numbers characterizing the vector nonet into a reasonable theoretical pattern, the “sore thumb” which sticks out is the $K^{*0} - K^{*+}$ mass difference. In ref. [7] a compromise fit was suggested to improve this prediction. Here we will show that, even if second order terms are included, this quantity can not be understood when other observables are fit exactly and when a conventional estimate is made for the photon exchange contribution. However, by deriving an analog of Dashen’s theorem[12] for electromagnetic contributions to the vector nonet isotopic spin violation splittings we demonstrate that there may be enough uncertainty to save this prediction.

All the parameters of our Lagrangian will be directly fitted from experimental data. This includes the pure pseudoscalar field piece for which both first and second order OZI rule conserving terms will be treated at tree level. The fit for those terms essentially reproduces the standard one[2]; even though the latter includes the finite parts of the one loop diagrams it doesn’t contribute much owing to the conventional choice of scale. In general, especially if there are many terms, it is difficult to practically distinguish finite loop corrections from higher order tree contributions. We will see that either can largely explain a 30% deviation of the $\rho^0 \rightarrow e^+e^-$ rate from its first order predicted value.

The leading symmetric terms of the effective Lagrangian are given in section 2.1. This section also contains the introduction of the (external) electroweak gauge bosons. We stress that the complete Lagrangian is gauge invariant by construction. Section 2.2 contains some discussion of different approaches to counting. We do not make a commitment to one counting scheme or another. However, we include enough terms to accommodate any reasonable scheme. We do separate the terms into these of OZI rule conserving and OZI rule violating type.

Section 3.1 discusses obtaining the parameters of the Lagrangian from experimental values of pseudoscalar masses and decay constants and vector meson masses and $V \rightarrow \phi\phi$ partial widths. The needed formulae are relegated, for the sake of readability, to Appendix A. The

specific effects of the OZI violation terms are discussed in section 3.2 (with some associated calculations described in Appendix B). It is noted that both an OZI violating, SU(3) conserving as well as an OZI violating, SU(3) violating piece are needed to fit the data. Of course, both effects are small and actually corrections due to isospin violations are shown not to be completely negligible.

The predictions for $\Gamma(\phi \rightarrow K\bar{K})$, $\Gamma(\omega \rightarrow \pi\pi)$, $\Gamma(\phi \rightarrow \pi\pi)$ and for the non electromagnetic piece of the $K^{*0}-K^{*+}$ mass difference are given in section 3.3 and Appendix C for each value of the quark mass ratio $x = 2m_s/(m_u + m_d)$. Setting $\Gamma(\omega \rightarrow \pi\pi)$ to its experimental value leads to a standard[13] determination of the quark mass ratios. It is also shown that relating the photon exchange piece of the $K^{*0}-K^{*+}$ mass difference to the $\rho^+-\rho^0$ mass difference permits a rather large uncertainty which may solve the $K^{*0}-K^{*+}$ puzzle. In section 3.4, the effects on the fitting of including second order symmetry breaking terms for the vectors is discussed. It does not seem to be possible to solve the $K^{*0}-K^{*+}$ puzzle in this way, however.

In section 4.1 we discuss the ρ^0 , ω and ϕ decays into e^+e^- . Even without symmetry breaking, vector meson dominance gives a reasonable, but not perfect, description of these processes. The effects of first order symmetry breaking terms unfortunately do not perfect the descriptions. Hence we introduce gauge invariant higher derivative photon–vector symmetry breaking terms which enable us to fit these decays exactly. Once again, a term which breaks both the OZI rule as well as SU(3) is seem to be important. We also remark that the $\rho^0 \rightarrow e^+e^-$ production can be improved by including the effect of the large rho width, as pointed out a long time ago[14]. It is noted that this can be understood as coming from pion loop corrections in the present framework.

Section 4.2 contains a discussion of the π^+ , K^+ and K^0 charge radii as well as the slope parameter of K_{e3} decay in our model. The terms just mentioned which improve the $V^0 \rightarrow e^+e^-$ predictions also improve the predictions for these quantities. Both $\Gamma(\omega \rightarrow \pi\pi)$ and $\Gamma(\rho \rightarrow e^+e^-)$ played an important role in our analysis. Actually these quantities are obtained from the experimental reaction $e^+e^- \rightarrow \pi^+\pi^-$. Thus we found it instructive to obtain the relevant Lagrangian parameters from directly fitting our theoretical formula for this reaction to experiment. This is discussed in section 4.3 and gives a feeling for the accuracy with which parameters characterizing a broad resonance like the ρ can be extracted from experiment.

2 Effective Lagrangian

Before proceeding to a detailed analysis of the symmetry breaking in the effective chiral Lagrangian of pseudoscalars plus vectors we shall, for the readers convenience, gather together here the terms which will actually be needed. We will include what we believe to be the leading terms which contribute to the vector meson masses and decay amplitudes. The terms proportional to the Levi-Civita symbol $\varepsilon_{\mu\nu\alpha\beta}$ will however not be discussed in the present paper.

2.1 The leading symmetric terms

These obey the chiral $U(3)_L \times U(3)_R$ symmetry. They will be also considered to obey the Okubo-Zweig-Iizuka (OZI or quark-line) rule[11] and to contain the minimum number of derivatives. Let us start with the $U(3)_L \times U(3)_R / U(3)_V$ nonlinear realization of chiral symmetry. The basic quantity is a 3×3 matrix U , which transforms as

$$U \rightarrow U_L U U_R^\dagger , \quad (2.1)$$

where $U_{L,R} \in U(3)_{L,R}$. This U is parametrized by the pseudoscalar nonet field ϕ as

$$U = \xi^2 , \quad \xi = e^{i\phi/F_\pi} , \quad (2.2)$$

where F_π is a “bare” pion decay constant. The vector nonet field ρ_μ is related to auxiliary linearly transforming “gauge fields” A_μ^L and A_μ^R by[15]

$$A_\mu^L = \xi \rho_\mu \xi^\dagger + \frac{i}{\tilde{g}} \xi \partial_\mu \xi^\dagger , \quad A_\mu^R = \xi^\dagger \rho_\mu \xi + \frac{i}{\tilde{g}} \xi^\dagger \partial_\mu \xi , \quad (2.3)$$

where \tilde{g} is a bare $\rho\phi\phi$ coupling. (For an alternative approach, which is equivalent at tree level, see ref. [16].) The symmetric terms may be expressed as[15]

$$\begin{aligned} \mathcal{L}_{\text{sym}} \equiv & -\frac{m_v^2(1+k)}{8k} \text{Tr} [A_\mu^L A_\mu^L + A_\mu^R A_\mu^R] + \frac{m_v^2(1-k)}{4k} \text{Tr} [A_\mu^L U A_\mu^R U^\dagger] \\ & - \frac{1}{4} \text{Tr} [F_{\mu\nu}(\rho) F_{\mu\nu}(\rho)] , \end{aligned} \quad (2.4)$$

where $F_{\mu\nu}(\rho)$ is the “gauge field strength” of vector mesons:

$$F_{\mu\nu}(\rho) = \partial_\mu \rho_\nu - \partial_\nu \rho_\mu - i\tilde{g}[\rho_\mu, \rho_\nu] . \quad (2.5)$$

Notice that $\text{Tr} [F_{\mu\nu}(A^L)F_{\mu\nu}(A^L)] = \text{Tr} [F_{\mu\nu}(A^R)F_{\mu\nu}(A^R)] = \text{Tr} [F_{\mu\nu}(\rho)F_{\mu\nu}(\rho)]$ so that (2.4) may be written directly in terms of the linearly transforming objects A_μ^L , A_μ^R and U . The parameter k is defined by

$$k \equiv \left(\frac{m_v}{\tilde{g}F_\pi} \right)^2 . \quad (2.6)$$

The choice $k = 2$ (which is well-known not to follow from the requirements of chiral symmetry) is called the Kawarabayashi-Suzuki-Riazuddin-Fayyazuddin (KSRF) relation[17] and turns out to be close to experiment. It is seen that the first two terms in (2.4), which each contain a factor of the degenerate vector meson mass parameter m_v , break the symmetry under *local* $U(3)_L \times U(3)_R$ transformations. We may make the entire Lagrangian locally gauge invariant by introducing a multiplet $B_\mu^{L,R}$ of external gauge fields which transforms in the same way as $A_\mu^{L,R}$ under local transformations. All that is required is the simple replacement:

$$A_\mu^{L,R} \rightarrow A_\mu^{L,R} - \frac{h}{\tilde{g}} B_\mu^{L,R} , \quad (2.7)$$

where h is an external field coupling constant. Of course, the last term in eq. (2.4) is already gauge invariant. The electroweak gauge fields (\mathcal{A}_μ : photon, \mathcal{Z}_μ and \mathcal{W}_μ : Z and W bosons) are embedded as

$$\begin{aligned} hB_\mu^L &= eQ\mathcal{A}_\mu + g_2 Q_Z \mathcal{Z}_\mu + \frac{g_2}{\sqrt{2}} (Q_W \mathcal{W}_\mu^+ + Q_W^\dagger \mathcal{W}_\mu^-) , \\ hB_\mu^R &= eQ\mathcal{A}_\mu - g_2 \frac{\sin^2 \theta_W}{\cos \theta_W} Q \mathcal{Z}_\mu , \end{aligned} \quad (2.8)$$

where

$$\begin{aligned} g_2 &= -e/\sin \theta_W , \\ Q &\equiv \begin{pmatrix} 2/3 & & \\ & -1/3 & \\ & & -1/3 \end{pmatrix} , \quad Q_W \equiv \begin{pmatrix} 0 & V_{ud} & V_{us} \\ 0 & 0 & 0 \\ 0 & 0 & 0 \end{pmatrix} , \\ Q_Z &\equiv \frac{1}{\cos \theta_W} \begin{pmatrix} 1/2 & & \\ & -1/2 & \\ & & -1/2 \end{pmatrix} - \frac{\sin^2 \theta_W}{\cos \theta_W} Q , \end{aligned} \quad (2.9)$$

with θ_W being the weak angle while V_{ud} and V_{us} are appropriate Kobayashi-Maskawa matrix elements. Notice that (2.8) and (2.9) refer only to the three light quark degrees of freedom and so do not include the light-heavy weak transition currents.

It is instructive to expand to leading order the terms linear in \mathcal{A}_μ which are obtained after substituting (2.7)–(2.9) into \mathcal{L}_{sym} of (2.4):

$$e\mathcal{A}_\mu \left[k\tilde{g}F_\pi^2 \text{Tr}(Q\rho_\mu) + i\left(1 - \frac{k}{2}\right) \text{Tr} \left[Q \left(\phi \overset{\leftrightarrow}{\partial}_\mu \phi \right) \right] \right] + \dots \quad (2.10)$$

We see that when $k = 2$, the direct single photon coupling to two charged pseudoscalars vanishes. Instead, the photon mixes with the neutral vector mesons according to the first term and the vector mesons then couple to two pseudoscalars. Hence, to the extent that k is experimentally equal to 2, a natural notion of vector meson dominance is automatic in this framework. By construction, the model is gauge invariant. Furthermore a transformation to the zero mass physical photon basis may be seen [16, 18] to give the identical results.

In writing (2.4) we considered only terms at most bilinear in A_μ^L and A_μ^R . Other symmetric terms with pieces such as $\text{Tr} [F_{\mu\nu}(A^L)A_\mu^L A_\mu^L]$, $\text{Tr} [A_\mu^L A_\mu^L A_\nu^L A_\nu^L]$ etc. are formally suppressed in the $1/N_c$ expansion.

2.2 Symmetry breaking terms

We next consider chiral $U(3)_L \times U(3)_R$ breaking terms which reflect the presence of non-zero quark masses in the fundamental QCD Lagrangian. We shall also consider terms which are not single traces in the $SU(3)$ flavor space and thereby violate the OZI rule.

The fundamental QCD Lagrangian contains the quark mass term $-\widehat{m}\bar{q}\mathcal{M}q$, where $\widehat{m} \equiv (m_u + m_d)/2$, and \mathcal{M} is the dimensionless matrix:

$$\mathcal{M} = \begin{pmatrix} 1+y & & \\ & 1-y & \\ & & x \end{pmatrix} \quad (2.11)$$

Here x and y are the quark mass ratios:

$$x = \frac{m_s}{\widehat{m}} \quad , \quad y = -\frac{1}{2} \left(\frac{m_d - m_u}{\widehat{m}} \right) \quad . \quad (2.12)$$

Another quantity of interest is

$$R = \frac{m_s - \widehat{m}}{m_d - m_u} = \frac{1-x}{2y} \quad . \quad (2.13)$$

We shall treat \mathcal{M} as a “spurion” which transforms like U in eq. (2.1). Then the symmetry breaking terms are *formally* chiral invariant.

The question of which symmetry breaking terms to include is, of course, a crucial one. First, consider the case when the vectors are absent. Then, the conventional approach is based on the chiral perturbation (ChPT) scheme[1, 2] in which one makes an expansion around threshold in such a way that two derivatives count the same as one appearance of \mathcal{M} . Then it seems that an adequate treatment of pseudoscalar masses and decay constants can be made by going to 4-derivative (or \mathcal{M}^2) order and choosing a scale in such a way that loop diagrams give negligible contributions. It is necessary to give special consideration to the very important OZI rule violation (U(1) problem) in the pseudoscalar multiplet — this was discussed in the present framework in sect. IV of ref. [7] and will not be repeated here. Apart from this, there are three OZI rule conserving, pseudoscalar-type symmetry breakers to order \mathcal{M}^2 . Specifically, at order \mathcal{M} there is one which is linear in the quark mass matrix without any derivatives, while at next order there is a quadratic in \mathcal{M} piece with no derivatives and a linear in \mathcal{M} piece with two derivatives. These are, as we will again see here, sufficient to reproduce the usual chiral perturbation theory fit to the pseudoscalar symmetry breaking parameters.

Now let us add the vectors. There is no immediately obvious counting scheme that will enable us to describe physics well away from $\pi\pi$ threshold. If there were it would amount to a practical solution of low energy QCD. However there are certainly useful clues to this problem. In the large N_c approximation of QCD the effective Lagrangian contains all nonet mesons and the leading approximation consists of keeping just the tree diagrams. In the low energy region this amounts to adding the vectors with presumably minimal derivative terms. The N_c expansion approach tends to replace the higher derivative pseudoscalar terms with the vectors. As far as symmetry breaking terms are concerned, it seems reasonable to emulate the pseudoscalar case and consider OZI rule conserving terms linear in \mathcal{M} with no derivatives, quadratic in \mathcal{M} with no derivatives and linear in \mathcal{M} with two derivatives. We shall see that there are considerably more than three terms of these types. Another approximation method is useful if we are mainly interested in soft pionic interactions of “on-shell” vector mesons. Then we may imagine the vectors to be heavy and make a chiral perturbation expansion around that point. For proper counting we should take the “heavy” vector to be moving with fixed 4-velocity V_μ and count the momentum as that of the “fluctuation” field $\rho'_\mu = e^{-im_\rho V \cdot x} \rho_\mu$. The resultant counting is similar to counting derivatives. Of course, considering the vectors as “heavy” is debatable. In any event, the terms we use will give rise

to the heavy field ones in the appropriate limit.*

Our initial model will contain the OZI rule conserving vector meson terms linear in \mathcal{M} , both with no derivatives and two derivatives. The vector meson terms of order \mathcal{M}^2 will be discussed separately. We only consider vector meson terms at most bilinear in the vector fields. Thus we write:

$$\begin{aligned}
\mathcal{L}_{\text{SB}} = & \alpha_1 \text{Tr} \left[\mathcal{M}^\dagger A_\mu^L U A_\mu^R + \mathcal{M} A_\mu^R U^\dagger A_\mu^L \right] \\
& + \alpha_2 \text{Tr} \left[U^\dagger \mathcal{M} U^\dagger A_\mu^L U A_\mu^R + U \mathcal{M}^\dagger U A_\mu^R U^\dagger A_\mu^L \right] \\
& + \frac{\alpha_3}{2} \text{Tr} \left[(\mathcal{M} U^\dagger + U \mathcal{M}^\dagger) A_\mu^L A_\mu^L + (\mathcal{M}^\dagger U + U^\dagger \mathcal{M}) A_\mu^R A_\mu^R \right] \\
& + \gamma' \text{Tr} \left[\mathcal{M}^\dagger F_{\mu\nu}^L U F_{\mu\nu}^R + \mathcal{M} F_{\mu\nu}^R U^\dagger F_{\mu\nu}^L \right] \\
& + \delta' \text{Tr} \left[\mathcal{M} U^\dagger + \mathcal{M}^\dagger U \right] \\
& + \lambda'^2 \text{Tr} \left[\mathcal{M} U^\dagger \mathcal{M} U^\dagger + \mathcal{M}^\dagger U \mathcal{M}^\dagger U - 2 \mathcal{M}^\dagger \mathcal{M} \right]. \tag{2.14}
\end{aligned}$$

The δ' term is the standard one for the pseudoscalar masses and the λ'^2 gives \mathcal{M}^2 corrections to it. The third purely pseudoscalar symmetry breaker of the type $\mathcal{M}\partial^2$ is, noting eq. (2.3), hidden in the α_i terms [see Appendix A.1]. There are two remaining independent non-derivative vector meson symmetry breaking combinations among the α_i terms corresponding to mass and $\rho\phi\phi$ coupling constant splittings. Previous fits[7, 8, 9, 10] of vector meson properties have only included a single linear combination of these. The new term noticeably improves the overall fit. Finally, the γ' term represents symmetry breaking in the vector meson kinetic terms. Another term of this type, obtained by replacing $\mathcal{M} \rightarrow U \mathcal{M}^\dagger U^\dagger$, is not independent as may be seen with the help of the relations, $F_{\mu\nu}^L = \xi F_{\mu\nu}(\rho) \xi^\dagger$ and $F_{\mu\nu}^R = \xi^\dagger F_{\mu\nu}(\rho) \xi$.

As previously noted, chiral counting and the inclusion of pion loops can be consistently done for pseudoscalars very close to the $\pi\pi$ threshold and also for very soft vector pion interactions wherein the vector remains close to its mass shell. However we shall initially restrict

* If $h = h' e^{iMV \cdot x}$ is a generic heavy boson field, the free Lagrangian $-\partial_\mu h \partial_\mu \bar{h} - M^2 h \bar{h}$ may be rewritten as $-iMV_\mu h' \overset{\leftrightarrow}{\partial}_\mu \bar{h}' + \dots$. This is the leading term of the “heavy” meson Lagrangian, which is to be expressed in terms of the field h' . A non derivative symmetry breaker (like the α_\pm terms of table 1) similarly gives rise to a term like $m_q M h' \mathcal{M} \bar{h}'$ which is counted of order quark mass m_q or momentum k^2 . A derivative type symmetry breaker (like the γ' term in eq. (2.14)) is rewritten as $\frac{m_q}{M} \partial_\mu h \mathcal{M} \overset{\leftrightarrow}{\partial}_\mu \bar{h} = -m_q M h' \mathcal{M} \bar{h}' + i m_q V_\mu h' \mathcal{M} \overset{\leftrightarrow}{\partial}_\mu \bar{h}' + \dots$. The first term on the right hand side has the same structure as the non derivative symmetry breaker. The second term on the right hand side has the same structure as an order k^3 term in the heavy meson counting. It is however formally suppressed by a factor $1/M$ compared to the leading terms. In practice, since the vectors are not very heavy, it plays the role of such a term.

ourselves to tree diagrams (as in the $1/N_c$ expansion) while using the effective Lagrangian in the extended low energy region up to about 1 GeV. Although we will not use it for our first fit, we give here the non-derivative \mathcal{M}^2 terms for the vectors:

$$\begin{aligned}
\mathcal{L}_\mu = & \mu_1 \text{Tr} \left[A_\mu^L \mathcal{M} A_\mu^R \mathcal{M}^\dagger \right] \\
& + \frac{\mu_2}{2} \text{Tr} \left[A_\mu^L U \mathcal{M}^\dagger U A_\mu^R \mathcal{M}^\dagger + A_\mu^R U^\dagger \mathcal{M} U^\dagger A_\mu^L \mathcal{M} \right] \\
& + \mu_3 \text{Tr} \left[A_\mu^L U \mathcal{M}^\dagger U A_\mu^R U^\dagger \mathcal{M} U^\dagger \right] \\
& + \frac{\mu_4}{2} \text{Tr} \left[A_\mu^L U \mathcal{M}^\dagger A_\mu^L \mathcal{M} U^\dagger + A_\mu^R U^\dagger \mathcal{M} A_\mu^R \mathcal{M}^\dagger U \right] \\
& + \frac{\mu_5}{4} \text{Tr} \left[A_\mu^L U \mathcal{M}^\dagger A_\mu^L U \mathcal{M}^\dagger + A_\mu^L \mathcal{M} U^\dagger A_\mu^L \mathcal{M} U^\dagger \right. \\
& \left. + A_\mu^R U^\dagger \mathcal{M} A_\mu^R U^\dagger \mathcal{M} + A_\mu^R \mathcal{M}^\dagger U A_\mu^R \mathcal{M}^\dagger U \right]. \quad (2.15)
\end{aligned}$$

We would also like to include terms which describe the small OZI rule violation in the vector nonet ($m_\omega - m_\rho \simeq 12\text{MeV}$ compared to $m_{K^*} - m_\rho \simeq 124\text{MeV}$). The terms which violate this rule but are nevertheless chiral symmetric take the form:

$$\mathcal{L}_{\nu 1} \equiv \nu_1 \left[(\text{Tr}[A_\mu^L])^2 + (\text{Tr}[A_\mu^R])^2 \right] + \nu_2 \text{Tr}[A_\mu^L] \text{Tr}[A_\mu^R]. \quad (2.16)$$

We also give the leading OZI violating terms[†] proportional to \mathcal{M} :

$$\begin{aligned}
\mathcal{L}_{\nu 2} \equiv & \nu_3 \left\{ \text{Tr}[A_\mu^L] \text{Tr}[A_\mu^L U \mathcal{M}^\dagger + A_\mu^L \mathcal{M} U^\dagger] + \text{Tr}[A_\mu^R] \text{Tr}[A_\mu^R U^\dagger \mathcal{M} + A_\mu^R \mathcal{M}^\dagger U] \right\} \\
& + \nu_4 \left\{ \text{Tr}[A_\mu^L] \text{Tr}[A_\mu^R U^\dagger \mathcal{M} + A_\mu^R \mathcal{M}^\dagger U] + \text{Tr}[A_\mu^R] \text{Tr}[A_\mu^L U \mathcal{M}^\dagger + A_\mu^L \mathcal{M} U^\dagger] \right\}. \quad (2.17)
\end{aligned}$$

One might expect, at first, the terms in $\mathcal{L}_{\nu 2}$ to be very much suppressed compared to those in $\mathcal{L}_{\nu 1}$. We will see later whether this, in fact, holds.

Linear combinations of the symmetry breaking parameters introduced in this section which naturally appear in the computation of physical quantities are listed in table 1. It should be stressed that the substitution (2.7) in all the terms above simply accomplishes the task of introducing electroweak interactions in a gauge invariant way.

[†] There exist two other terms which violate the OZI rule and break SU(3) symmetry: $\text{Tr}[U \mathcal{M}^\dagger + U^\dagger \mathcal{M}] \text{Tr}[A_\mu^L A_\mu^L + A_\mu^R A_\mu^R]$, $\text{Tr}[U \mathcal{M}^\dagger + U^\dagger \mathcal{M}] \text{Tr}[A_\mu^L U A_\mu^R U^\dagger]$. However, for the physical quantities studied in this paper, (vector meson masses, $\rho\pi\pi$ coupling and so on), these effects are absorbed into the coefficients of the symmetric terms in eq. (2.4). Hence we do not include such terms explicitly.

α_+	$\alpha_1 + \alpha_2 + \alpha_3$
α_-	$\alpha_1 - \alpha_2$
α_p	$\alpha_1 + \alpha_2 - \alpha_3$
μ_a	$\mu_1 + \mu_2 + \mu_3 + \mu_4 + \mu_5$
μ_b	$\mu_1 - \mu_2 + \mu_3 + \mu_4 - \mu_5$
μ_c	$\mu_1 + \mu_2 + \mu_3 - \mu_4 - \mu_5$
μ_d	$\mu_1 - \mu_2 + \mu_3 - \mu_4 + \mu_5$
μ_e	$\mu_1 - \mu_3$
ν_a	$2\nu_1 + \nu_2$
ν_b	$4\nu_3 + 4\nu_4$
ν_c	$2\nu_1 - \nu_2$
ν_d	$4\nu_3 - 4\nu_4$

Table 1: Convenient parameter combinations.

3 Observable Quantities of the Model

In this section we discuss the physical quantities computed from the Lagrangian

$$\mathcal{L} = \mathcal{L}_{\text{sym}} + \mathcal{L}_{\text{SB}} + \mathcal{L}_{\nu 1} + \mathcal{L}_{\nu 2} . \quad (3.1)$$

Altogether we consider 13 *a priori* unknown parameters. At the level of the symmetric piece \mathcal{L}_{sym} , there are only three quantities: m_v , \tilde{g} and the “bare” pion decay constant F_π . Adding symmetry breaking brings in the two quark mass ratios x and y . Our analysis yields, as a byproduct, an alternative extraction of these fundamental quantities from experiment. There are three OZI rule conserving symmetry breaking coefficients (δ' , λ'^2 and α_p) associated with the pure pseudoscalar sector and three more OZI rule conserving but symmetry breaking coefficients (α_+ , α_- and γ') resulting from the addition of vectors. Two coefficients (ν_a and ν_b) describing OZI rule violation for the vector multiplet bring the total to thirteen.

The results of computing the needed physical quantities and related discussions are presented in Appendix A.

3.1 Parameter fitting

The introduction of symmetry breaking terms requires us to renormalize the various fields. First, we consider the isospin symmetric limit by setting $y = 0$ in the breaking term \mathcal{M} . The

α_p -term and γ' -term give contributions to the kinetic terms of the pseudoscalar mesons and the vector mesons, respectively. Then taking typical examples:

$$\begin{aligned}\pi^+ &\equiv Z_\pi \phi_{12}, \quad K^+ \equiv Z_K \phi_{13}, \\ \rho_\mu^+ &= Z_\rho \rho_{12\mu}, \quad K_\mu^{*+} = Z_{K^*} \rho_{13\mu}, \quad \omega_\mu = Z_\omega (\rho_{11\mu} + \rho_{22\mu})/\sqrt{2}, \quad \phi_\mu = Z_\phi \rho_{33\mu}.\end{aligned}\quad (3.2)$$

The explicit forms of the normalization constants are shown in eqs. (A.7) and (A.8). The renormalizations of the pseudoscalar fields imply that physical pion and kaon decay constants $F_{\pi p}$ and F_{Kp} are also renormalized as

$$F_{\pi p} = Z_\pi F_\pi, \quad F_{Kp} = Z_K F_\pi. \quad (3.3)$$

We will determine the parameters of the model using the most well known quantities namely the particle masses, ρ and K^* decay widths[‡] and the decay constants of (3.3). At first we neglect OZI rule violations; it will be discussed separately in the next subsection. The inputs are displayed in table 2. All but one of them will (for our present purpose) have negligible errors. However, the non-electromagnetic piece of the K^0 – K^+ mass difference, contains the error shown[13] associated with the theoretical estimation of the photon exchange piece.

vector meson masses and partial widths (MeV)					
m_ρ	m_ω	m_{K^*}	m_ϕ	$\Gamma(\rho \rightarrow \pi\pi)$	$\Gamma(K^* \rightarrow K\pi)$
769.9	781.9	893.8	1019.4	151.2	49.8

pseudoscalar meson masses and decay constants(MeV)				
m_π	m_K	$[\Delta m_K]_{\text{nonEM}}$	$F_{\pi p}$	F_{Kp}
137.3	495.7	5.27 ± 0.30	130.7	159.8

Table 2: The physical inputs used for fitting. The values are listed in the Particle Data Group [19].

The pion and kaon masses are obtained by expanding the δ' and λ'^2 terms:

$$\begin{aligned}m_\pi^2 &= \frac{8}{F_{\pi p}^2} (\delta' + 4\lambda'^2), \\ m_K^2 &= \frac{4}{F_{Kp}^2} [(1+x)\delta' + 2(1+x)^2\lambda'^2].\end{aligned}\quad (3.4)$$

[‡] Actually as discussed on p. 1456 of ref. [19], the precise values of mass, width etc. for very broad resonances depend to some extent on the method of parameterization. See also section 4.3 of the present paper.

The contributions to the vector meson masses (see eq. (A.9)) and the $\rho\phi\phi$ coupling constants (see eqs. (A.15)–(A.19)) come from the α_+ , α_- and ν terms. The theoretical expression for $[\Delta m_K]_{\text{nonEM}}$ is finally given in eq. (A.10).

First, we determine the values of all parameters for various fixed values of x . Using the physical values of the two decay constants F_{Kp} and $F_{\pi p}$, we determine α_p/\tilde{g}^2 and F_π^2 . The parameters m_v , α_+ and γ' are determined from the vector meson masses m_ρ , m_{K^*} and m_ϕ . Next, the parameters α_- and \tilde{g} are determined from the widths $\Gamma(\rho \rightarrow \pi\pi)$ and $\Gamma(K^* \rightarrow K\pi)$. The isospin breaking parameter y is finally determined from the non-electromagnetic part of the K^0-K^+ mass difference. We list the values of parameters in table 3 for each choice of x . (We list also the quark mass ratio $R = (1-x)/(2y)$.) It should be remarked that

x	y	R	$\gamma' \times 10^{-3}$	$\alpha_+^\dagger \times 10^{-3}$	$\alpha_-^\dagger \times 10^{-3}$	$\alpha_p^\dagger \times 10^{-3}$	$\delta'^{\dagger\dagger} \times 10^{-3}$	$ \lambda' ^\dagger \times 10^{-3}$	m_v (GeV)	\tilde{g}	F_π (GeV)
14	-0.12	54.1	0.419	-7.23	-0.684	5.27	0.0304	1.57	0.75	4.03	0.126
17	-0.155	51.5	0.345	-5.87	-0.542	4.3	0.0344	1.21	0.753	4.04	0.127
20.5	-0.202	48.2	0.29	-4.81	-0.432	3.54	0.0369	0.916	0.756	4.04	0.127
23	-0.241	45.6	0.264	-4.25	-0.375	3.15	0.038	0.755	0.758	4.05	0.128
26	-0.295	42.4	0.241	-3.73	-0.32	2.77	0.0388	0.597	0.759	4.05	0.128
29	-0.358	39.2	0.225	-3.32	-0.276	2.48	0.0394	0.464	0.761	4.05	0.128
32	-0.433	35.8	0.214	-2.98	-0.24	2.24	0.0398	0.343	0.761	4.05	0.129

Table 3: The values of parameters determined from the experimental data. The unit of the quantities indicated by \dagger ($\dagger\dagger$) is $(\text{GeV})^2$ ($(\text{GeV})^4$).

the numerical values in table 3 already include the corrections obtained when fitting in the presence of OZI rule violation.

In our model the following generalization of the Gell-Mann–Okubo mass formula holds:

$$Z_\phi^2 m_\phi^2 = 2Z_{K^*}^2 m_{K^*}^2 - Z_\rho^2 m_\rho^2 , \quad (3.5)$$

Actually, in our fit, Z_ϕ , Z_{K^*} and Z_ρ do not differ too much from unity. (Noting that $Z_{K^*}^2 = (Z_\phi^2 + Z_\rho^2)/2$, we see that the ratio Z_ϕ/Z_ρ is independent of parameter choice.) In an earlier fit[7] larger deviations of Z_ϕ and Z_{K^*} from unity (corresponding to larger choices for x) were considered in an attempt to explain the puzzling value of the non-electromagnetic piece of the $K^{*0}-K^{*+}$ mass difference. Here we will show that the electromagnetic contribution to $K^{*0}-K^{*+}$ may be more uncertain than previously thought. (see section 3.3)

As one might expect, the parameters m_v , \tilde{g} and F_π of the symmetric Lagrangian turn out not to depend much on x . We will find a best value of x by later examining predictions of the model. Notice that the α_- coefficient turns out to be only about 1/10 of α_+ . α_+ contributes to both mass and coupling constant splittings while α_- contributes only to coupling constant splittings. This shows that both types of splittings are approximately controlled by the parameter α_+ . This may be understood by noting from eqs. (A.9) and (A.16) that $\alpha_- \neq 0$ corresponds to a deviation from the formula $g_{\rho\pi\pi} = m_\rho^2 / (\tilde{g} F_{\pi p}^2)$.

3.2 OZI rule violation for the vector nonet

Historically the OZI rule was discovered in trying to understand the vector meson nonet, which emphasizes that these violating effects are small. The ν_a term in eq. (A.6) yields SU(3) symmetric OZI rule violation while the ν_b term yields SU(3) non-symmetric OZI rule violation. We will fit these two parameters from $m_\omega - m_\rho$ and from an *experimentally determined* $\omega\phi$ mixing angle. The latter is defined from

$$\begin{pmatrix} \omega_\mu \\ \phi_\mu \end{pmatrix} = \begin{pmatrix} \cos \theta_{\phi\omega} & \sin \theta_{\phi\omega} \\ -\sin \theta_{\phi\omega} & \cos \theta_{\phi\omega} \end{pmatrix} \begin{pmatrix} \omega_{p\mu} \\ \phi_{p\mu} \end{pmatrix}, \quad (3.6)$$

where the subscript p denotes the physical field. Furthermore our convention (see eq. (3.2)) sets ω_μ and ϕ_μ to be the “ideally mixed” fields. Hence the mixing angle $\theta_{\phi\omega}$ will be very small. It can be seen from eq. (A.9) that $m_\omega - m_\rho$ determines the combination $(\nu_a + \nu_b)$ while eq. (A.13) shows that the mixing angle will determine the combination $2\nu_a + (1+x)\nu_b$. First it is interesting to see what $\theta_{\phi\omega}$ would be if ν_b were absent. Then we may calculate

$$\theta_{\phi\omega} \simeq \frac{\Pi_{\phi\omega}}{m_\phi^2 - m_\omega^2} = \frac{m_\omega^2 - m_\rho^2}{m_\phi^2 - m_\omega^2} \sqrt{\frac{m_\phi^2 - m_{K^*}^2}{2m_{K^*}^2 - 3m_\rho^2 + m_\omega^2}} \simeq 0.0325, \quad (3.7)$$

where the relation

$$\left(\frac{Z_\phi}{Z_\rho}\right)^2 = \frac{m_{K^*}^2 - (3m_\rho^2 - m_\omega^2)/2}{m_\phi^2 - m_{K^*}^2} \quad (3.8)$$

was used. While the numerical value of $\theta_{\phi\omega}$ in eq. (3.7) has the right order of magnitude, it turns out to be only about 60% of the value needed to explain the branching ratio $\Gamma(\phi \rightarrow \pi^0\gamma)/\Gamma(\omega \rightarrow \pi^0\gamma)$ using a model based on the mixing approximation.[§] Inclusion of the ν_b term can lead to experimental agreement. The relevant Feynman diagram is shown in fig. 1,

[§] It seems plausible to neglect the effects of a direct OZI violating term of the form $\varepsilon_{\mu\nu\alpha\beta} \text{Tr}(\partial_\mu \rho_\nu) \text{Tr}(\partial_\alpha \rho_\beta \phi)$, which could lead to $\phi \rightarrow \pi^0 \rho \rightarrow \pi^0 \gamma$.

along with an iso-spin violating one which gives a 10% correction. It is amusing that iso-spin violations may be non-negligible; this is due to the smallness of OZI rule violation. The calculation is discussed in Appendix B. The iso-spin violating correction depends on x and this leads to a small x dependence for the “experimentally obtained” value of $\theta_{\phi\omega}$. As x

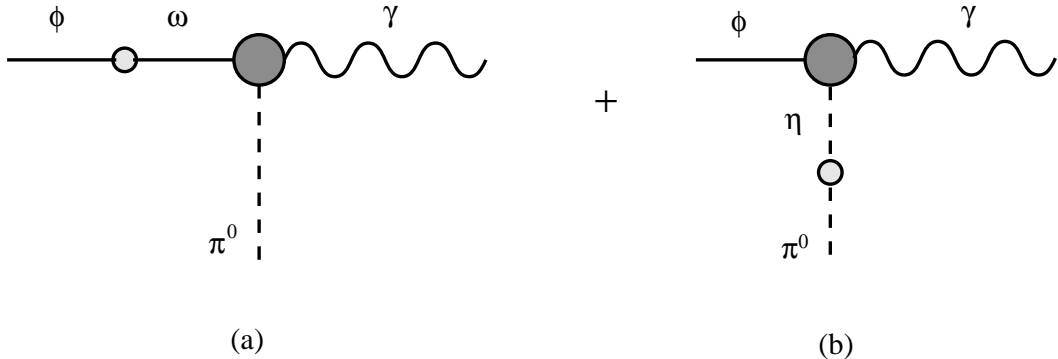


Figure 1: Feynman diagrams describing the contributions to $\phi \rightarrow \pi^0\gamma$ decay from (a) $\phi\text{-}\omega$ mixing and (b) $\pi^0\text{-}\eta$ mixing.

varies from 14 to 32, $\theta_{\phi\omega}$ varies from 0.056 to 0.052 radians. The choice $x = 20.5$ leads to the OZI rule violating parameters

$$\begin{aligned} \nu_a &= -4.29 \times 10^{-3} \text{GeV}^2, \\ \nu_b &= -0.357 \times 10^{-3} \text{GeV}^2. \end{aligned} \quad (3.9)$$

While ν_b makes a small contribution to $m_\omega - m_\rho$, it actually (because it gets multiplied by x) makes a very substantial contribution to $\theta_{\phi\omega}$. It thus appears that the product (OZI violation) \times (SU(3) symmetry breaking) is not suppressed for the vector nonet as one might initially expect.

Among the parameters shown in table 3, only γ' and α_- have a non-negligible dependence on OZI violation. These dependences are illustrated, for $x = 20.5$, in table 4. Also shown are the effects on some physical observables which will be discussed later.

3.3 Predictions

So far we used up most of the vector meson masses and widths just to determine the coefficients of the Lagrangian (3.1) for any x . However, there are several physical masses and widths left over which we can predict and compare with experiment. This will also

	$\gamma' \times 10^{-3}$	$\alpha_- \times 10^{-3}(\text{GeV})^2$	Z_ϕ	$[\text{Br}(\phi)]_{\pi\pi} \times 10^{-4}$	$\Gamma(\omega \rightarrow e^+e^-)$ (KeV)	$\langle r_{K^0}^2 \rangle$ (fm) ²
(a)	0.905	0.0964	0.923	0	0.583	-0.0150
(b)	0.660	-0.112	0.944	0.116	0.638	-0.00877
(c)	0.290	-0.432	0.976	0.869	0.682	-0.00141

Table 4: The dependence of the parameters and physical observables on the OZI violating parameters ν_a and ν_b . We show the values for (a) $\nu_a = \nu_b = 0$; (b) $\nu_a \neq 0$ and $\nu_b = 0$; (c) $\nu_a \neq 0$ and $\nu_b \neq 0$ with $x = 20.5$ fixed.

enable us to choose the value of x . The leftover masses are the non-electromagnetic parts of $\Delta m_{K^*} \equiv m(K^{*0}) - m(K^{*+})$ and the ρ^0 - ω and ρ^0 - ϕ transition masses. These actually contribute to the $\omega \rightarrow 2\pi$ and $\phi \rightarrow 2\pi$ decays according to the diagram of fig. 2(a). In the present model there are also direct $\omega \rightarrow 2\pi$ and $\phi \rightarrow 2\pi$ vertices as shown in fig. 2(b). Another predicted three point vertex describes $\Gamma(\phi \rightarrow K\bar{K})$; in this case there is also a

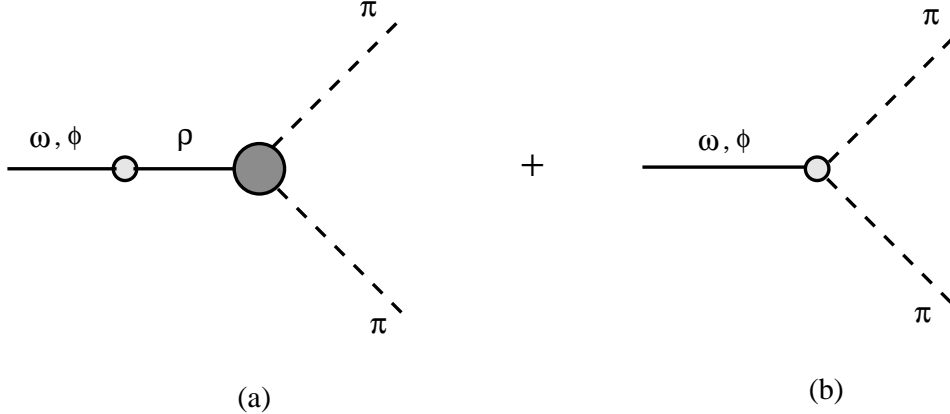


Figure 2: Feynman diagrams describing the contributions to $\omega(\phi) \rightarrow \pi\pi$ decay from (a) ρ^0 - ω (ϕ) mixing and (b) direct $\omega\pi\pi$ ($\phi\pi\pi$) vertex.

correction corresponding to $\phi \rightarrow \omega \rightarrow K\bar{K}$.

We give the predictions for $\Gamma(\phi \rightarrow K\bar{K})$, $\Gamma(\omega \rightarrow \pi\pi) / \Gamma(\rho \rightarrow \pi\pi)$ and the non-electromagnetic part of the K^{*0} - K^{*+} mass difference Δm_{K^*} in table 5. We include the OZI rule violating ν terms, which generate the ρ - ϕ mixing and the direct $\phi\pi\pi$ coupling, in our fit. Also shown is the predicted branching ratio $\Gamma(\phi \rightarrow \pi\pi) / \Gamma(\phi \rightarrow \text{all})$.

First consider the prediction for $\Gamma(\phi \rightarrow K\bar{K})$. It is seen to be in reasonably good agree-

x	$\Gamma(\phi \rightarrow K\bar{K})$ (MeV)	$[M_{\rho\omega}]_{\text{nonEM}}$ (MeV)	$g_{\omega\pi\pi}$	$[\Gamma(\omega)/\Gamma(\rho)]_{\pi\pi}$ $\times 10^{-3}$	$[\Delta m_{K^*}]_{\text{nonEM}}$ (MeV)	$[\text{Br}(\phi)]_{\pi\pi}$ $\times 10^{-4}$
14	3.52	-2.51	-0.0525	0.95	2.18	0.717
17	3.52	-2.63	-0.0550	1.06	2.29	0.78
20.5	3.52	-2.81	-0.0585	1.24	2.45	0.869
23	3.52	-2.96	-0.0616	1.41	2.59	0.944
26	3.52	-3.18	-0.0659	1.65	2.79	1.05
29	3.52	-3.44	-0.0709	1.97	3.02	1.17
32	3.53	-3.75	-0.0769	2.39	3.31	1.31
expt.	3.69 ± 0.06			1.23 ± 0.19		$(0.8^{+0.8}_{-0.4})$

Table 5: Predictions.

ment with experiment and also to be essentially independent of x . This can be understood by noting that in the case $\nu_a = \nu_b = 0$, we have the following relation among $\rho\phi\phi$ couplings:

$$g_{\phi K\bar{K}} = 2g_{K^*K\pi} \left(\frac{F_{\pi p}}{F_{Kp}} \right) \left(\frac{Z_{K^*}}{Z_\phi} \right) - g_{\rho\pi\pi} \left(\frac{F_{\pi p}}{F_{Kp}} \right)^2 \left(\frac{Z_\rho}{Z_\phi} \right) . \quad (3.10)$$

Each ratio of two Z 's is independent of parameter choice, as discussed below eq. (3.5). Then we obtain $\Gamma(\phi \rightarrow \pi\pi) = 3.71$ (MeV) independently of x for $\nu_a = \nu_b = 0$. When we include the small OZI rule violating terms, this relation is only slightly changed.

Next consider the $\omega \rightarrow \pi\pi$ process. Details of the calculation are given in Appendix C. Examining table 5 shows that the result depends sensitively on x and that the experimental value $\Gamma(\omega \rightarrow \pi\pi)/\Gamma(\rho \rightarrow \pi\pi) = 1.23$ selects

$$x = 20.5 , \quad R = 48.2 , \quad [M_{\rho\omega}]_{\text{nonEM}} = -2.81 \text{ (MeV)} . \quad (3.11)$$

Now from table 3 we read off $y = -0.202$ and hence that the fundamental quark masses are estimated to stand in the ratio

$$m_u : m_d : m_s = 1 : 1.51 : 25.7 . \quad (3.12)$$

It turns out that the effect of the direct $\omega \rightarrow 2\pi$ vertex, which had not been considered in previous discussions, is small. This may be understood in the following way. If we neglect the small effect from γ' in $M_{\rho\omega}$ and the small deviation from the relation $g_{\rho\pi\pi} = m_\rho^2/(\tilde{g}F_{\pi p}^2)$, the ratio of the mass mixing and direct contributions is estimated in terms of the ratio of ρ

meson mass to width as

$$\left(\frac{M_{\rho\omega}}{\Gamma_\rho/2}\right)^2 : \left(\frac{g_{\omega\pi\pi}}{g_{\rho\pi\pi}}\right)^2 \simeq \left(\frac{-4y\alpha_+}{m_\rho\Gamma_\rho}\right)^2 : \left(\frac{-4y\alpha_+}{m_\rho^2}\right)^2 \simeq \left(\frac{m_\rho}{\Gamma_\rho}\right)^2 : 1 \simeq 26 : 1. \quad (3.13)$$

[Using the values shown in table 5 we find $(2M_{\rho\omega}/\Gamma_\rho)^2 : (g_{\omega\pi\pi}/g_{\rho\pi\pi})^2 \simeq 30 : 1$.] In the present model the following relation between vector meson masses and ρ - ω mixing is satisfied when the OZI violating ν terms are neglected:

$$[M_{\rho\omega}]_{\text{nonEM}} = -\frac{1}{R} \frac{m_{K^*}^2 - m_\rho^2}{2m_\rho} \left(\frac{Z_{K^*}}{Z_\rho}\right)^2. \quad (3.14)$$

This is similar to the relation derived in ref. [13]. Thus our value in eq. (3.11) is close to the value in ref. [13].

From table 5 we observe that the predicted branching ratio $\Gamma(\phi \rightarrow \pi\pi)/\Gamma(\phi \rightarrow \text{all})$ (see Appendix C for details) for $x = 20.5$ agrees well with the central experimental value. However the experimental error is large.

Our final prediction of this type is seen from table 5 to be

$$[\Delta m_{K^*}]_{\text{nonEM}} = 2.45 \text{ MeV}. \quad (3.15)$$

This number may be roughly understood from the predicted ratio which holds with $\nu_a = \nu_b = 0$:

$$\frac{[\Delta m_{K^*}]_{\text{nonEM}}}{-[M_{\rho\omega}]_{\text{nonEM}}} = \frac{m_\rho}{m_{K^*}} \left(\frac{Z_\rho}{Z_{K^*}}\right)^4 \simeq 1.0. \quad (3.16)$$

On the other hand, the Particle Data Group[19] tells us that

$$\Delta m_{K^*} = \begin{cases} 4.5 \pm 0.4 \text{ MeV} & \text{(a)} \\ 6.7 \pm 1.2 \text{ MeV} & \text{(b)} \end{cases}, \quad (3.17)$$

depending on whether one (a) simply subtracts the listed K^{*+} mass from the listed K^{*0} mass or (b) considers just the “dedicated” experiments. In order to compare this with our prediction it is necessary to take the electromagnetic piece $[\Delta m_{K^*}]_{\text{EM}}$, defined by

$$\Delta m_{K^*} = [\Delta m_{K^*}]_{\text{nonEM}} + [\Delta m_{K^*}]_{\text{EM}} \quad (3.18)$$

into account. A bag model estimate[20] gave $[\Delta m_{K^*}]_{\text{EM}} = -0.7 \text{ MeV}$. Thus, and this is an old puzzle, there appears to be a serious disagreement. In a previous paper[7], this motivated a compromise fit in which x was much larger (since $[\Delta m_{K^*}]_{\text{nonEM}}$ increases with increasing x)

but $m(\phi)$ was allowed to differ somewhat from its experimental value. In the next subsection we will investigate the effect of the \mathcal{M}^2 , μ -type terms on this puzzle.

Now, however, we would like to see what a “model-independent” estimate for $[\Delta m_{K^*}]_{\text{EM}}$ has to say on this matter. For the pseudoscalars one usually employs such an approach[¶] (i.e., Dashen’s theorem[12]) to estimate the analogous quantity $[\Delta m_K]_{\text{EM}}$. For the vectors we may derive a sum rule for the electromagnetic parts of the mass differences by assuming the OZI rule in the form that the vector field appears as a nonet and the effective operator is a single trace. Corresponding to photon exchange we should have two powers of Q (defined in eq. (2.9)). The effective operator describing the electromagnetic contributions to the mass splittings then takes the form

$$A \text{Tr} (Q\rho_\mu Q\rho_\mu) + B \text{Tr} (Q^2 \rho_\mu \rho_\mu) , \quad (3.19)$$

where A and B are some constants. This leads to the sum rule:

$$[\Delta m_{K^*}]_{\text{EM}} = [m(K^{*0}) - m(K^{*+})]_{\text{EM}} = \frac{m_\rho}{m_{K^*}} \left[[m(\rho^0) - m(\rho^+)]_{\text{EM}} - [M_{\rho\omega}]_{\text{EM}} \right] . \quad (3.20)$$

$[M_{\rho\omega}]_{\text{EM}}$ has (see eq. (C.2)) been estimated as 0.42MeV. Furthermore, since $m(\rho^0) - m(\rho^+)$ is a $\Delta I = 2$ object, it is a good approximation to neglect the quark mass ($\Delta I = 1$ at first order) contribution and set

$$[m(\rho^0) - m(\rho^+)]_{\text{EM}} \simeq [m(\rho^0) - m(\rho^+)] = 0.3 \pm 2.2 \text{ MeV} , \quad (3.21)$$

where the PDG[19] estimate was used in the last step. We thus get the desired estimate

$$[\Delta m_{K^*}]_{\text{EM}} = -0.11 \pm 1.9 \text{ MeV} . \quad (3.22)$$

With our prediction for $[\Delta m_{K^*}]_{\text{nonEM}}$ we would then have

$$\Delta m_{K^*} = 2.34 \pm 1.9 \text{ MeV} . \quad (3.23)$$

This value has a large enough uncertainty to possibly agree with the experimental value in eq. (3.17.a) above. In any event, the large uncertainty associated with the $\rho^+ - \rho^0$ experimental mass splitting suggests a certain skepticism about accepting literally the stated $K^{*0} - K^{*+}$ experimental value.

[¶] In our present language, Dashen’s theorem amounts to the observation that the only non derivative effective operator which agrees with the chiral transformation property of the product of two electromagnetic currents is $\tilde{U}_{11}\tilde{U}_{11}^\dagger = (4/F_\pi^2)(\pi^+\pi^- + K^+K^-) + \dots$. This gives $\Delta m_\pi^\gamma = \Delta m_K^\gamma$. Here $U = U_0\tilde{U}$ with $\det\tilde{U} = 1$.

3.4 Second Order Effects

In this section we study the effects of the μ -labeled, \mathcal{M}^2 symmetry breakers for the vector meson nonet. These are given in eq. (2.15) and rewritten in terms of convenient linear combinations in eq. (A.5). (Note that the formulas listed in Appendix A contain the μ -term contributions.) The motivation for this study is to see if we can fit the model to a larger value for $[\Delta m_{K^*}]_{\text{nonEM}}$, which could be required by future precision experiments. Without the μ -terms (and neglecting the OZI violating ν -terms), eq. (3.16) shows that $[\Delta m_{K^*}]_{\text{nonEM}}$ can not be any greater than $-[M_{\rho\omega}]_{\text{nonEM}}$ when all the input parameters are fit exactly. We now have a similar relation in the presence of the μ -terms. Still keeping $\nu_a = \nu_b = 0$ and using the formulae given in Appendix A we find

$$\left[\frac{\Delta m_{K^*}}{-M_{\rho\omega}} \right]_{\text{nonEM}} = \frac{m_\rho}{m_{K^*}} \times \frac{m_\phi^2 - m_{K^*}^2}{m_{K^*}^2 - m_\rho^2} \times \frac{Z_\rho^2 Z_\phi^2}{Z_{K^*}^4} < 1.0. \quad (3.24)$$

To get the final inequality, we used $(Z_\rho Z_\phi)/(Z_{K^*}^2) = 2(Z_\rho Z_\phi)/(Z_\rho^2 + Z_\phi^2) \leq 1$. When we include the OZI violating ν_a and ν_b terms, the relation (3.24) is slightly changed to:

$$\left[\frac{\Delta m_{K^*}}{-M_{\rho\omega}} \right]_{\text{nonEM}} = \frac{m_\rho}{m_{K^*}} \times \frac{Z_\rho^2}{Z_{K^*}^2} \times \frac{Z_\phi^2(m_\phi^2 - m_{K^*}^2) + Z_\rho^2(m_\omega^2 - m_\rho^2)/2 - Z_\rho Z_\phi(\sqrt{2}\Pi_{\phi\omega})}{Z_{K^*}^2(m_{K^*}^2 - m_\rho^2) - Z_\rho^2(m_\omega^2 - m_\rho^2)/2 + Z_\rho Z_\phi(\sqrt{2}\Pi_{\phi\omega})/2}. \quad (3.25)$$

In order to evaluate this expression we should fit the Lagrangian parameters including the μ terms. We shall set $\mu_c = 0$ since it only affects the pseudoscalar decay constants. μ_b and μ_d do not contribute to the quantities discussed in this paper. We shall fit μ_a and μ_e to the experimental values of the $\phi \rightarrow K\bar{K}$ and $\omega \rightarrow \pi\pi$ decay widths (these two quantities are thus no longer predictions). The quark mass ratio x will be kept fixed at 20.5. It is then convenient to consider parameters evaluated for various values of Z_ϕ (see eq. (A.8)). These are shown in table 6. We next show the dependence of $[\Delta m_{K^*}/M_{\rho\omega}]_{\text{nonEM}}$ on Z_ϕ for $x = 20.5$ in fig. 3. Here we use as an input, $\theta_{\phi\omega}$ as derived from $\phi \rightarrow \pi^0\gamma$ decay width for x around 20.5 in section 3.2. It is clear from Fig. 3 that $[\Delta m_{K^*}]_{\text{nonEM}}$ is still approximately bounded by $-[M_{\rho\omega}]_{\text{nonEM}}$. If a more precise experimental value of Δm_{K^*} turns out in the 5 KeV range it would be difficult to explain in this model as arising from $[\Delta m_{K^*}]_{\text{nonEM}}$ – a suitably large value of $[\Delta m_{K^*}]_{\text{EM}}$ would be required.

In table 6 we also show predictions for the ρ^0 , ω and ϕ decay widths into e^+e^- . These will be discussed in more detail in the next section. Here we just want to point out that getting agreement with experiment does in fact require Z_ϕ to be within about $\pm 25\%$ of unity.

Z_ϕ	μ_a	μ_e	m_v	\tilde{g}	α_+	α_-	$V \rightarrow e^+e^-$		
	$\times 10^{-3}$	$\times 10^{-3}$	(GeV)		$\times 10^{-3}$	$\times 10^{-3}$	$\Gamma(\rho)$	$\Gamma(\omega)$	$\Gamma(\phi)$
0.5	0.204	-0.00227	0.761	4.15	2.01	2.75	4.80	0.583	0.314
0.8	0.0994	-0.0186	0.759	4.10	-1.78	1.08	5.03	0.638	0.875
1.0	-0.000542	0.00417	0.756	4.03	-5.28	-0.676	5.28	0.689	1.44
1.1	-0.0595	0.0241	0.755	3.99	-7.33	-1.80	5.44	0.720	1.79
1.5	-0.355	0.153	0.747	3.75	-17.4	-8.25	6.49	0.905	3.85

Table 6: The dependences of the parameters on Z_ϕ for $x = 20.5$. The units of the parameters μ_a , μ_e , α_+ and α_- are $(\text{GeV})^2$. The predictions for $V \rightarrow e^+e^-$ are also shown. [The units are (KeV).]

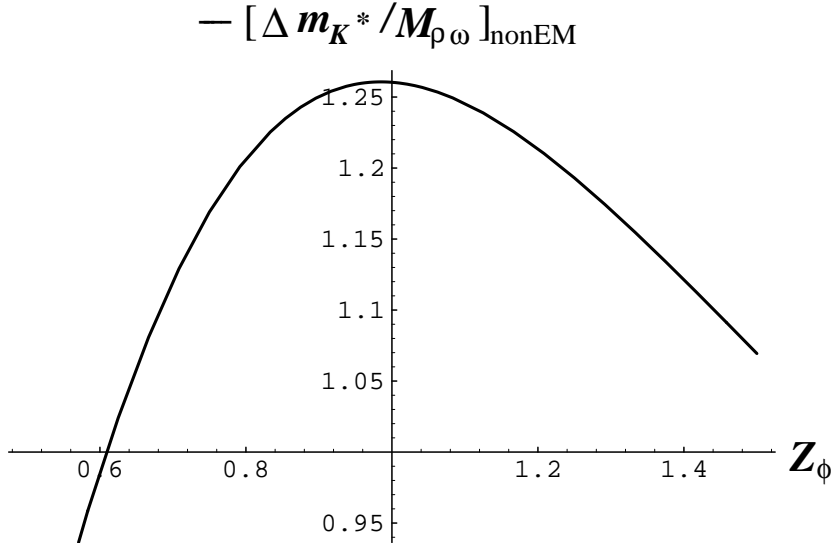


Figure 3: The dependence of the ratio $[\Delta m_{K^*}/M_{\rho\omega}]_{\text{nonEM}}$ on Z_ϕ for $x = 20.5$. We use $\theta_{\phi\omega} = 0.055$.

4 Electroweak Processes

In the previous section we determined the parameters of the effective Lagrangian for various values of the quark mass ratio, x . Some predictions were also made and a best value of x around 20 was selected. All the physical quantities discussed were independent of the electroweak gauge fields. In this section we will study processes which are related to the electroweak interaction. The electroweak gauge fields may be introduced, without introducing any new arbitrary constants, according to the prescription of (2.7)–(2.9). Using our Lagrangian, we will first give predictions for the $V \rightarrow l^+l^-$ ($V = \rho, \omega, \phi$; $l = e, \mu$) decays. Next, we calculate form factors; namely the pion and kaon charge radii as well as the slope parameter of K_{e3} decay. Finally, we will discuss a direct fit of the experimental $e^+e^- \rightarrow \pi^+\pi^-$ data using our Lagrangian. This provides a consistency check as well as an indication of what is involved in obtaining vector meson parameters from experiment.

4.1 $V \rightarrow e^+e^-$ decay processes

Let us write the effective Lagrangian describing the $V-\gamma$ transition terms in our model as:

$$\mathcal{L}_{V\gamma} \equiv e\mathcal{A}_\mu [g_\rho\rho_\mu + g_\omega\omega_\mu + g_\phi\phi_\mu] . \quad (4.1)$$

The expressions for the transition strengths g_ρ , g_ω and g_ϕ are given in eq. (A.20). In terms of these transition strengths the $V \rightarrow l^+l^-$ decay widths are given by

$$\Gamma(V \rightarrow l^+l^-) = \frac{4\pi\alpha^2}{3} \left| \frac{g_{Vp}}{M_V^2} \right|^2 \frac{M_V^2 + 2m_l^2}{M_V^2} \sqrt{M_V^2 - 4m_l^2} , \quad (4.2)$$

where

$$g_{\rho_p} = g_\rho , \quad g_{\omega_p} = g_\omega - \theta_{\phi\omega}g_\phi , \quad g_{\phi_p} = g_\phi + \theta_{\phi\omega}g_\omega . \quad (4.3)$$

Here we included the $\phi-\omega$ mixing from the OZI rule violating terms $\mathcal{L}_{\nu 1} + \mathcal{L}_{\nu 2}$.

Before calculating the partial widths, we note some relations between the ratios of these partial widths and the vector meson masses. In the case where $\nu_a = \nu_b = 0$, the relation

$$\frac{g_\rho}{m_\rho^2} = 3 \frac{g_\omega}{m_\omega^2} = -\frac{3}{\sqrt{2}} \frac{Z_\rho}{Z_\phi} \frac{g_\phi}{m_\phi^2} = \frac{Z_\rho}{\sqrt{2}\tilde{g}} \quad (4.4)$$

is satisfied. Noting that the values of Z_ρ and Z_ϕ depend on x while their ratio, according to the discussion around eq. (3.5), depends only on masses we find the following x -independent

relations:

$$\frac{g_\omega}{g_\rho} = \frac{1}{3} \frac{m_\omega^2}{m_\rho^2}, \quad -\frac{g_\phi}{g_\omega} = \sqrt{2} \frac{m_\phi^2}{m_\rho^2} \frac{Z_\phi}{Z_\rho} \simeq 2.2. \quad (4.5)$$

From these relations we obtain $\Gamma(\omega \rightarrow e^+e^-)/\Gamma(\rho \rightarrow e^+e^-) \simeq 0.11$ and $\Gamma(\phi \rightarrow e^+e^-)/\Gamma(\omega \rightarrow e^+e^-) \simeq 2.2$. These ratios are in reasonable agreement with the experimental values given by 0.09 and 2.3, respectively.

Now, including the OZI violation terms we calculate the decay widths using the parameters determined in the previous section and display them in table 7. It is seen that the

x	$V \rightarrow e^+e^-$			
	$\Gamma(\rho)$	$\Gamma(\omega)$	$\Gamma(\phi)$	$\Gamma(\rho)_{\text{GS}}^\dagger$
14	5.28	0.688	1.37	6.31
17	5.26	0.685	1.37	6.29
20.5	5.24	0.682	1.36	6.27
23	5.23	0.680	1.36	6.26
26	5.23	0.678	1.35	6.25
29	5.22	0.676	1.35	6.24
32	5.21	0.673	1.35	6.24
exp.	6.77 ± 0.32	0.60 ± 0.02	1.37 ± 0.05	6.77 ± 0.32

Table 7: The predictions for $V \rightarrow l^+l^-$ decay widths in units of KeV. $\Gamma(\rho)_{\text{GS}}$ indicates that the Gounaris-Sakurai[14] effect is included (see text).

x -dependences are quite small. The predicted value for the ϕ decay agrees well with experiment, while the ω meson prediction is about 10% too high and the ρ meson prediction is about 25% too low. Let us consider the last point in detail. In our model, the ratio of $\Gamma(\rho \rightarrow e^+e^-)$ to $\Gamma(\rho \rightarrow \pi^+\pi^-)$ is given by

$$R_{e\pi} \equiv \frac{\Gamma(\rho \rightarrow e^+e^-)}{\Gamma(\rho \rightarrow \pi^+\pi^-)} = \frac{\alpha^2}{36} \left| \frac{m_\rho^2 - 4m_\pi^2}{m_\rho^2} \right|^{3/2} \left(\frac{m_\rho}{\Gamma_\rho} \right)^2 \left(\frac{g_\rho g_{\rho\pi\pi}}{\sqrt{2}m_\rho^2} \right)^2. \quad (4.6)$$

Since the contribution from the α_- term to $g_{\rho\pi\pi}$ is very small, the KSRF relation $2m_\rho^2 = g_{\rho\pi\pi}^2 F_\pi^2$ ^{||} means the last factor in eq. (4.6) is very close to unity, i.e., $g_\rho \simeq \sqrt{2}m_\rho^2/g_{\rho\pi\pi}$. Then the predicted value of the $\rho \rightarrow e^+e^-$ decay width is seen to be somewhat small compared with the experimental value.

^{||} Experimentally, $(2m_\rho^2)/(g_{\rho\pi\pi}^2 F_\pi^2) \simeq 0.957$. This form of the KSRF relation agrees with the choice $k = 2$ in eq. (2.6) when symmetry breaking is neglected.

A natural way to fine tune our predictions is to include gauge invariant, higher derivative ρ – γ transition terms. Let us introduce the following effective Lagrangian terms which describe the “kinetic type” ρ – γ transitions:

$$\begin{aligned}
\mathcal{L}_{V\gamma} = & h\kappa_0 \text{Tr} \left[F_{\mu\nu}(\rho) \left\{ \xi F_{\mu\nu}^R(B) \xi^\dagger + \xi^\dagger F_{\mu\nu}^L(B) \xi \right\} \right] \\
& + h \frac{\kappa_1}{2} \text{Tr} \left[\left\{ \widehat{\mathcal{M}}_+, F_{\mu\nu}(\rho) \right\} \left(\xi F_{\mu\nu}^R(B) \xi^\dagger + \xi^\dagger F_{\mu\nu}^L(B) \xi \right) \right] \\
& + h \frac{\kappa_2}{2} \text{Tr} \left[\left[\widehat{\mathcal{M}}_-, F_{\mu\nu}(\rho) \right] \left(\xi F_{\mu\nu}^R(B) \xi^\dagger - \xi^\dagger F_{\mu\nu}^L(B) \xi \right) \right] \\
& + h\kappa_3 \text{Tr} [F_{\mu\nu}(\rho)] \text{Tr} [F_{\mu\nu}^R(B) + F_{\mu\nu}^L(B)] \\
& + h\kappa_4 \text{Tr} [\widehat{\mathcal{M}}_+ F_{\mu\nu}(\rho)] \text{Tr} [F_{\mu\nu}^R(B) + F_{\mu\nu}^L(B)] \\
& + h\kappa_5 \text{Tr} [F_{\mu\nu}(\rho)] \text{Tr} \left[\widehat{\mathcal{M}}_+ \left(\xi F_{\mu\nu}^R(B) \xi^\dagger + \xi^\dagger F_{\mu\nu}^L(B) \xi \right) \right]
\end{aligned} \tag{4.7}$$

where $\widehat{\mathcal{M}}_\pm$ is defined in eq. (A.2). The κ_0 term is the leading kinetic type mixing term while the κ_1 and κ_2 terms describe the first order symmetry breaking pieces which conserve the OZI rule. The κ_3 term describes the OZI rule violating contribution to the ρ – γ mixing and the first order symmetry breaking and OZI rule violating pieces are given by the κ_4 and κ_5 terms. Noting that $\text{Tr}(Q) = 0$ and that $\widehat{\mathcal{M}}_-$ must include at least one pseudoscalar meson, we see that only the κ_0 , κ_1 and κ_5 terms contribute to the kinetic type ρ – γ mixing without pseudoscalar mesons. Let the C_V denote kinetic type ρ – γ mixing coefficients in the effective Lagrangian:*

$$\mathcal{L}_{V\gamma \text{kin}} = e(\partial_\mu \mathcal{A}_\nu - \partial_\nu \mathcal{A}_\mu) \left[C_\rho \partial_\mu \rho_\nu^0 + C_\omega \partial_\mu \omega_\nu + C_\phi \partial_\mu \phi_\nu \right] . \tag{4.8}$$

The C_V are then given by

$$\begin{aligned}
C_\rho &= \frac{4}{\sqrt{2}Z_\rho} [\kappa_0 + \kappa_1] , \\
C_\omega &= \frac{4}{3\sqrt{2}Z_\omega} [\kappa_0 + \kappa_1 - 2(x-1)\kappa_5] , \\
C_\phi &= -\frac{4}{3Z_\phi} [\kappa_0 + x\kappa_1 + (x-1)\kappa_5] .
\end{aligned} \tag{4.9}$$

These kinetic mixing terms are included by replacing g_{Vp} by $g_{Vp} - C_{Vp} M_V^2$ in eq. (4.2), where we also take the ϕ – ω mixing into account.

* In ref. [21] such a term has been advocated to fit all the V – γ mixing, rather than just the corrections to eq. (4.1).

We determine the values of these parameters from the experimental e^+e^- decay widths and obtain

$$C_\rho \simeq -0.024, \quad C_\omega \simeq 0.0039, \quad C_\phi \simeq 0.00005, \quad (4.10)$$

for $x = 20.5$. [The variations of C_ρ and C_ω are less than 5% for a wide range of x -values ($14 \leq x \leq 45$). The range of C_ϕ is $-0.00027 \sim 0.001$ for $14 \leq x \leq 45$.] The large difference between C_ρ and C_ω implies that the κ_5 term gives a contribution which is comparable to the leading order one; $2x\kappa_5 \sim \kappa_0$. The κ_5 term is expected to be suppressed by the OZI rule in addition to the smallness of the SU(3) symmetry breaking mass. A similar effect was observed in section 3.2. We should notice that the main contribution to the $\rho-\gamma$ transition is supplied by the mass type mixing g_V , the value of which is determined from the pure hadronic sector and is almost consistent with the experiment. In other words, the plausible KSFR relation $g_\rho = \sqrt{2}m_\rho^2/g_{\rho\pi\pi}$ is naturally explained by the mass type mixing, and small corrections are given by the kinetic type mixing. For the ρ meson case, the kinetic type mixing gives about a 15% correction to the mass type mixing amplitude in order to achieve agreement with experiments.

Another possibility for improving the $\Gamma(\rho^0 \rightarrow e^+e^-)$ prediction is to take the large ρ width into account, as Gounaris and Sakurai pointed out long ago[14]. They included the finite width corrections based on a generalized effective range formula for pion-pion scattering and got a non-negligible enhancement factor for the pion form factor:

$$F_\pi(s) = \frac{m_\rho^2 + dm_\rho\Gamma_\rho}{(m_\rho^2 - s) + \Pi(s) - im_\rho\Gamma_\rho(k/k_\rho)^3(m/\sqrt{s})}, \quad (4.11)$$

where

$$\begin{aligned} \Pi(s) &= \Gamma_\rho \frac{m_\rho^2}{k_\rho^3} \left[k^2 \left\{ h(s) - h(m_\rho^2) \right\} + k_\rho^2 h'(m_\rho^2)(m_\rho^2 - s) \right], \\ h(s) &= \frac{2}{\pi} \frac{k}{\sqrt{s}} \ln \left(\frac{\sqrt{s} + 2k}{2m_\pi} \right), \quad k = \sqrt{\frac{s - 4m_\pi^2}{4}}, \quad k_\rho = \sqrt{\frac{m_\rho^2 - 4m_\pi^2}{4}}, \\ d &= \frac{3}{\pi} \frac{m_\pi^2}{k_\rho^2} \ln \left(\frac{m_\rho + 2k_\rho}{2m_\pi} \right) + \frac{m_\rho}{2\pi k_\rho} - \frac{m_\pi^2 m_\rho}{\pi k_\rho^3}. \end{aligned} \quad (4.12)$$

As a result the above ratio (4.6) is enhanced to

$$R_{e\pi}|_{\text{finite width}} = R_{e\pi} \times [1 + d(\Gamma_\rho/m_\rho)]^2. \quad (4.13)$$

In our model this effect is included by the replacement

$$g_\rho \rightarrow g_\rho \times [1 + d(\Gamma_\rho/m_\rho)], \quad (4.14)$$

which enhances the predicted value of $\Gamma(\rho \rightarrow e^+ e^-)$ by about 20%. We show the result of this enhancement in the fifth column in table 7. Clearly, this G-S effect improves the prediction. It should be noticed that the inclusion of the pion loop correction to the ρ propagator and to the $\rho\pi\pi$ coupling with a suitable (vector) on-shell-like renormalization (we need a higher derivative counter term) gives the same result as the G-S form factor.

4.2 Charge radii and the slope factor of K_{e3}

We now consider the pion and kaon charge radii and also the slope factor of K_{e3} decay. In our model the electromagnetic charge radius of the pseudoscalar P is expressed as

$$\langle r_P^2 \rangle = \frac{6}{\sqrt{2}} \sum_V \frac{g_{Vp}^{PP} g_{Vp}}{M_V^4} , \quad (4.15)$$

where $V = (\rho, \omega, \phi)$. When we include the kinetic type $\rho\gamma$ mixing, the above g_{Vp} 's are replaced with $g_{Vp} - C_{Vp} M_V^2$. The slope factor of K_{e3} decay is defined by the linear energy dependence of the form factor f_+ in the matrix element of $K \rightarrow \pi l \nu$ decay:

$$\begin{aligned} \mathcal{M} &\propto f_+(t) \left[(p_K + p_\pi)_\mu \bar{l} \gamma_\mu (1 + \gamma_5) \nu \right] + f_-(t) m_l \bar{l} (1 + \gamma_5) \nu , \\ f_+(t) &= f_+(0) \left[1 + \lambda_+(t/m_\pi^2) \right] . \end{aligned} \quad (4.16)$$

In our model this form factor is dominated by the K^* meson exchange diagram. Then λ_+ is expressed as

$$\frac{\lambda_+}{m_\pi^2} = \frac{2F_{Kp}F_{\pi p}}{F_{Kp}^2 + F_{\pi p}^2} \frac{g_{K^*} g_{K^* K\pi}}{\sqrt{2} m_{K^*}^4} , \quad (4.17)$$

where $g_{K^*} = \sqrt{2} Z_{K^*} m_{K^*}^2 / \tilde{g}$ is the K^* – W transition strength defined by

$$\mathcal{L}_{K^*W} = \frac{g_2}{4} g_{K^*} \left(V_{us} K_\mu^{*-} \mathcal{W}_\mu^+ + V_{us}^* K_\mu^{*+} \mathcal{W}_\mu^- \right) . \quad (4.18)$$

When we include the kinetic type $\rho\gamma$ transition terms as given in eq. (4.7), this also gives a kinetic type K^* – W transition term:

$$\mathcal{L}_{K^*W\text{kin}} = \frac{g_2}{4} C_{K^*} \left[V_{us} \left(\partial_\mu \mathcal{W}_\nu^+ - \partial_\nu \mathcal{W}_\mu^+ \right) \partial_\mu K_\nu^{*-} + V_{us}^* \left(\partial_\mu \mathcal{W}_\nu^- - \partial_\nu \mathcal{W}_\mu^- \right) \partial_\mu K_\nu^{*+} \right] , \quad (4.19)$$

where C_{K^*} is given by

$$C_{K^*} = \frac{2\sqrt{2}}{Z_{K^*}} [2\kappa_0 + (x+1)\kappa_1] . \quad (4.20)$$

This effect is included in the slope parameter λ_+ by the replacement $g_{K^*} \rightarrow g_{K^*} - C_{K^*} m_{K^*}^2$ in eq. (4.17).

We show our predictions for the charge radii and the slope parameter in table 8 together with the existing experimental values. The dependence on the parameter x is very small as is the case for the partial width $\Gamma(V \rightarrow e^+e^-)$. Thus we show only the prediction for $x = 20.5$. (Actually, the variation of the predictions for different values of x is less than 0.5%.) In the first line we use the ρ - γ transition strengths given in eqs. (4.3) and (A.20), while in the second line we include the kinetic type ρ - γ mixing corrections as discussed in the previous section. Here we used the values of the C_V 's determined from the e^+e^- partial decay widths. It is reassuring that the corrections discussed in section 4.1 to improve $\Gamma(V \rightarrow e^+e^-)$ also improve the predictions in table 8.

	$\langle r_\pi^2 \rangle$ (fm) 2	$\langle r_{K^+}^2 \rangle$ (fm) 2	$\langle r_{K^0}^2 \rangle$ (fm) 2	λ_+
Prediction 1	0.415	0.260	-0.00141	0.0257
Prediction 2	0.472	0.275	-0.0221	0.0264
Prediction 3	0.424	0.263	-0.00467	
Molzon (1978)[22]			- (0.054 ± 0.026)	
Dally (1977)[23]	0.31 ± 0.04			
Dally (1980)[24]		0.28 ± 0.05		
Dally (1982)[25]	0.439 ± 0.030			
Amendolia (1984)[26]	0.432 ± 0.016			
Barkov (1985)[27]	0.422 ± 0.013			
Amendolia (1986)[28]		0.34 ± 0.05		
Amendolia (1986)[29]	0.439 ± 0.008			
Erkal (1987)[30]	0.455 ± 0.005	0.29 ± 0.04		
PDG (1994)[19]				0.0286 ± 0.0022

Table 8: Predictions for the charge radii and the K_{e3} slope parameter λ_+ with the existing experimental values. The values on the second line (Prediction 2) are given by the inclusion of the kinetic type ρ - γ transition strength as shown in eq. (4.9). The values in the third line (Prediction 3) include the enhancement factor due to the replacement (4.21).

When we take the finite ρ width into account, the pion form factor is changed as given in eq. (4.11). Since $\Pi(s)$ in eq. (4.12) does not affect the form factor on the vector meson mass shell while it does near $s = 0$, the replacement (4.14) is not valid for the charge radii.

Instead, the following replacement is obtained in the low energy region:

$$g_\rho \rightarrow g_\rho \times \frac{1 + \tilde{d}(\Gamma_\rho/m_\rho)}{1 + d(\Gamma_\rho/m_\rho)},$$

$$\tilde{d} = \frac{m_\rho^2 + 2m_\pi^2}{2\pi k_\rho^2} \ln \left(\frac{m_\rho + 2k_\rho}{2m_\pi} \right) + \frac{m_\rho}{2\pi k_\rho} - \frac{m_\rho^3}{3\pi k_\rho^3}. \quad (4.21)$$

We show in the third line of table 8 the predictions gotten by this replacement. The predictions are only slightly improved by the inclusion of the G-S effect.

Finally we make a comment on the K^0 charge radius and the γ' symmetry breaking term in eq. (2.14). Using the first order ($\nu_a = \nu_b = 0$) formula given in appendix A, we find

$$\begin{aligned} \langle r_{K^0}^2 \rangle &= -\frac{8(x+1)}{\tilde{g}^2 F_{Kp}^2} \left[\gamma' + \frac{\alpha_-}{2} \left(\frac{1}{m_\rho^2} - \frac{1}{m_\phi^2} \right) \right] \\ &\simeq -\frac{8(x+1)\gamma'}{\tilde{g}^2 F_{Kp}^2} \simeq -0.01 \text{ (fm)}^2, \end{aligned} \quad (4.22)$$

where in the second line we neglected symmetry breaking terms of quadratic order such as $\alpha_+ \times \alpha_-$. This shows that the inclusion of the γ' term is important for the charge radius of K^0 . However, since the first order mass relation (3.5) suppresses γ' , we obtain a smaller value than the experimental one. When we include either the G-S-like enhancement factor with the replacement (4.14), or the kinetic type mixing C_V , the negative ρ contribution is enhanced and the prediction is improved (more substantially in the kinetic mixing case).

4.3 $e^+e^- \rightarrow \pi\pi$ process

In section 4.1 we determined the value of the coefficient of the kinetic type $\rho-\gamma$ mixing C_ρ from the experimental value of $\Gamma(\rho \rightarrow e^+e^-)$. We used the decay width $\Gamma(\omega \rightarrow \pi\pi)$ to fit x in section 3.3. These two decay processes are related to the $e^+e^- \rightarrow \pi\pi$ process. In this section we directly fit C_ρ and x from the experimental data describing the pion form factor of $e^+e^- \rightarrow \pi\pi$ [27] in the energy region $0.73 \leq \sqrt{s} \leq 0.83$ (GeV). The restriction of the energy region reduces the dependence on effects which are difficult to calculate reliably.

In the present model there exist four kinds of contributions to the pion form factor. We show the corresponding Feynman diagrams in fig. 4. Figure 4(a) represents the contribution from the direct $\gamma\pi\pi$ coupling $g_{\gamma\pi\pi}$. In the present model this is expressed as

$$g_{\gamma\pi\pi} = 1 - \frac{Z_\rho}{2\tilde{g}} g_{\rho\pi\pi} + y \frac{2\alpha_+}{3\tilde{g}^2 F_{\pi p}^2}, \quad (4.23)$$

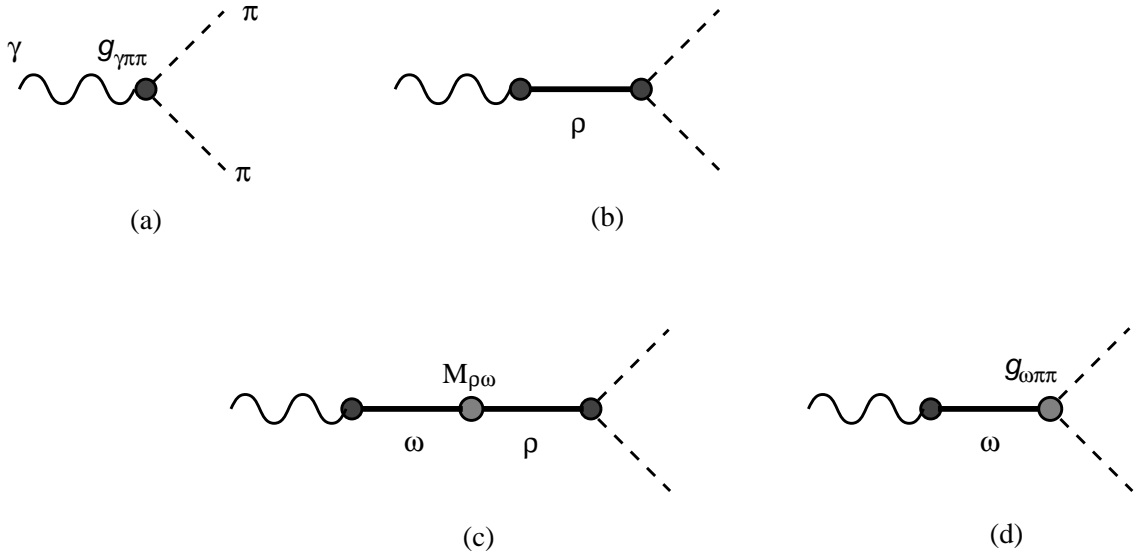


Figure 4: The Feynman diagrams contributing to the pion form factor: (a) the direct $\gamma\pi\pi$ vertex; (b) the ρ meson exchange diagram; (c) the ρ - ω mixing; (d) the direct $\omega\pi\pi$ vertex.

where we also included the term proportional to the iso-spin violating quark mass ratio y . The contribution from the ρ - ω mixing is shown in fig. 4(c). In section 3.3, we concentrated on the on-shell region and used an effective momentum independent ρ - ω mixing. However, here we consider the momentum dependence of the form factor, including the momentum dependence which comes from the kinetic type ρ - ω mixing provided by the γ' term as^{††}

$$M_{\rho\omega}(s) = \frac{-y}{m_\rho Z_\rho^2} [2\alpha_+ + \nu_b - 4\gamma' s] + [M_{\rho\omega}]_{\text{EM}} . \quad (4.24)$$

Figure 4(d) shows the contribution from the direct $\omega\pi\pi$ coupling $g_{\omega\pi\pi}$, as discussed in section 3.3.

Adding the above four contributions, the pion form factor is given by

$$\begin{aligned} F(s) = & g_{\gamma\pi\pi} + \frac{g_{\rho\pi\pi}}{\sqrt{2}}(g_\rho - C_\rho s)D_\rho(s) - \frac{g_{\rho\pi\pi}}{\sqrt{2}}(g_{\omega_p} - C_{\omega_p} s)(2m_\rho M_{\rho\omega}(s))D_\rho(s)D_\omega(s) \\ & + \frac{g_{\omega\pi\pi}}{\sqrt{2}}(g_{\omega_p} - C_{\omega_p} s)D_\omega(s) , \end{aligned} \quad (4.25)$$

where $D_V(s)$ ($V = \rho, \omega$) is the vector meson propagator:

$$D_V(s) = \frac{1}{M_V^2 - s - iM_V\Gamma_V(s)} . \quad (4.26)$$

^{††} Even if we use the momentum independent ρ - ω mixing, the results in this section are not changed much since the energy region is restricted to that near the ρ and ω mass shells.

Here we use a momentum dependent ρ meson width but neglect this effect for the much narrower ω meson:

$$\begin{cases} \Gamma_\rho(s) = \left(\frac{s - 4m_\pi^2}{m_\rho^2 - 4m_\pi^2} \right)^{3/2} \frac{m_\rho}{\sqrt{s}} \theta(s - 4m_\pi^2) \Gamma_\rho, \\ \Gamma_\omega(s) = \Gamma_\omega. \end{cases} \quad (4.27)$$

The parameters in the form factor except for C_ρ and C_{ω_p} are determined from the physical quantities shown in table 2 together with the ϕ - ω mixing angle $\theta_{\phi\omega}$ for fixed x . [The value of $\theta_{\phi\omega}$ affects the quantities in the form factor (4.25) through the parameter ν_b .] We determine the value of C_{ω_p} from the experimental value of $\Gamma(\omega \rightarrow e^+e^-)$ for each x as discussed in section 4.1. In the previous sections, we used the experimental value of $\Gamma(\phi \rightarrow \pi^0\gamma)$ to determine the ϕ - ω mixing angle for fixed x including the π^0 - η mixing effect. We fitted the parameter ν_b with this angle $\theta_{\phi\omega}$. Here, to avoid complexity and to check the dependence on this angle, we fix $\theta_{\phi\omega} = 0.055$ or 0.0325 . The former value is determined from the $\phi \rightarrow \pi^0\gamma$ decay width in section 3.2 for x around 20.5, while the latter is given in the case $\nu_b = 0$ as shown in eq. (3.7). There are furthermore experimental and theoretical errors in the value of the non-electromagnetic part of the $K^+ - K^0$ mass difference $[\Delta m_K]_{\text{nonEM}}$, which is used to determine y for fixed x . We will take this uncertainty into account by using variously $[\Delta m_K]_{\text{nonEM}} = 5.27, 4.97$ and 5.57 (MeV) as inputs.

First, we show the best fitted curve for $\theta_{\phi\omega} = 0.055$ and $[\Delta m_K]_{\text{nonEM}} = 5.27$ (MeV) in fig. 5. This shows that our model fits experiment well in the energy region where the ρ and ω mesons are close to their mass shell.

Next, we show the best fitted values of C_ρ and x in table 9 for the choices of $\theta_{\phi\omega}$ and $[\Delta m_K]_{\text{nonEM}}$ mentioned above. We also show the values of $g_{\gamma\pi\pi}$, C_ω , R , $[M_{\rho\omega}]_{\text{nonEM}} \equiv M_{\rho\omega}(s = m_\rho^2) - [M_{\rho\omega}]_{\text{EM}}$ and the branching ratio $\Gamma(\omega \rightarrow \pi\pi)/\Gamma(\rho \rightarrow \pi\pi)$. As is expected, the contribution from the direct $\gamma\pi\pi$ vertex is small compared with the ρ meson exchange contribution: even in the low energy limit, the ρ meson exchange diagram gives $g_\rho g_{\rho\pi\pi}/(\sqrt{2}m_\rho^2) \simeq 1.05$, while the direct $\gamma\pi\pi$ vertex gives $g_{\gamma\pi\pi} \simeq -0.05$.

The best fitted value of C_ρ does not depend on $\theta_{\phi\omega}$ and $[\Delta m_K]_{\text{nonEM}}$ very much. On the other hand, the calculated value of C_ω does depend on $\theta_{\phi\omega}$. For all cases, the absolute value of C_ρ is larger than that of C_ω . In other words, C_ω is much suppressed compared with C_ρ . This implies that the κ_5 term in the kinetic type ρ - γ mixing terms (see eqs. (4.7) and (4.10)), which violates the OZI rule and breaks SU(3) symmetry at the same time, gives a non-negligible contribution, as discussed in section 4.1.

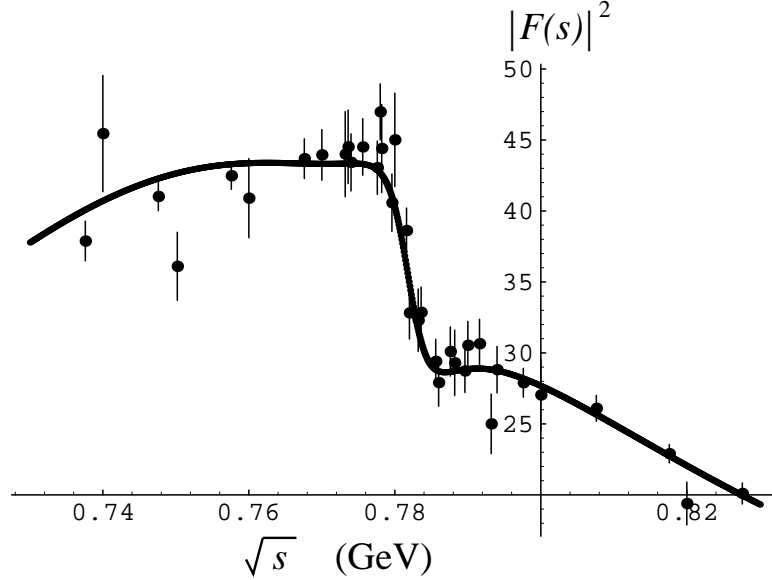


Figure 5: The best fitted curve for $\theta_{\phi\omega} = 0.055$ and $[\Delta m_K]_{\text{nonEM}} = 5.27(\text{MeV})$. The best fitted values of C_ρ and x are -0.0303 and 17.2 , respectively. The experimental data is given in ref. [27].

$\theta_{\phi\omega}$	$[\Delta m_K]_{\text{nonEM}}$ (MeV)	C_ρ	x	$g_{\gamma\pi\pi}$	C_ω	R	$[M_{\rho\omega}]_{\text{nonEM}}$ (MeV)	$[\Gamma(\omega)/\Gamma(\rho)]_{\pi\pi}$ $\times 10^{-3}$
0.055	4.97	-0.0306	20.2	-0.051	0.0039	51.4	-2.63	1.07
	5.27	-0.0303	17.2	-0.052	0.0040	51.4	-2.63	1.07
	5.57	-0.0300	13.8	-0.054	0.0041	51.4	-2.63	1.07
0.0325	4.97	-0.0312	23.3	-0.046	0.0019	48.0	-2.64	1.06
	5.27	-0.0312	20.7	-0.046	0.0019	48.0	-2.65	1.06
	5.57	-0.0311	17.9	-0.047	0.0019	48.0	-2.65	1.06

Table 9: The best fitted values of C_ρ and x . The calculated values of $g_{\gamma\pi\pi}$, C_ω , R , $[M_{\rho\omega}]_{\text{nonEM}}$ and the branching ratio $\Gamma(\omega \rightarrow \pi\pi)/\Gamma(\rho \rightarrow \pi\pi)$ are also shown.

The best fitted value of x depends on the choice of input values of $\theta_{\phi\omega}$ and $[\Delta m_K]_{\text{nonEM}}$. However, the non-electromagnetic part of the strength of ρ - ω mixing $[M_{\rho\omega}]_{\text{nonEM}}$ is very stable against the choice of input parameters:

$$[M_{\rho\omega}]_{\text{nonEM}} = -2.63 \sim -2.65 \text{ (MeV)} . \quad (4.28)$$

The estimated value of the quark mass ratio R does not depend on the choice of $[\Delta m_K]_{\text{nonEM}}$, while it depends slightly on the ϕ - ω mixing angle $\theta_{\phi\omega}$. The value of R for $\theta_{\phi\omega} = 0.055$ is

$$R = 51.4 , \quad (4.29)$$

which is larger than the best fitted value given in section 3.3. However, if we take the error of the experimental value of $\omega \rightarrow \pi\pi$ decay width into account, these two fits agree with each other. [The calculated value of $\Gamma(\omega \rightarrow \pi\pi)/\Gamma(\rho \rightarrow \pi\pi)$ is 1.07×10^{-3} ; on the other hand, experimentally it is $(1.23 \pm 0.19) \times 10^{-3}$.]

Finally, we make a comment on the uncertainty of the ρ meson mass. Since the ρ meson has a broad width compared to ω and ϕ , there is an uncertainty as to the precise value of its mass. Actually the best fitted value given in ref. [27] is $m_\rho = 775.9$ (MeV). If we fit the ρ meson mass in addition to C_ρ and x , we obtain the following best fitted values for $\theta_{\phi\omega} = 0.055$ and $[\Delta m_K]_{\text{nonEM}} = 5.27$ (MeV):

$$C_\rho = -0.0310 , \quad x = 23.1 , \quad m_\rho = 774 \text{ (MeV)} . \quad (4.30)$$

These lead to $R = 45.5$ and $\Gamma(\omega \rightarrow \pi\pi)/\Gamma(\rho \rightarrow \pi\pi) = 1.31 \times 10^{-3}$. This R agrees with the previous fit in section 3.3, if we include the experimental error for $\Gamma(\omega \rightarrow \pi\pi)/\Gamma(\rho \rightarrow \pi\pi)$.

This analysis shows that x has an uncertainty of about ± 3 . Furthermore, it indicates the close connection between the precise values of parameters extracted from experiment and the model used to analyze the experiment. It is clear that obtaining greater precision in the future will require that different experiments be analyzed with the same theoretical model.

5 Discussion

For many purposes it is extremely useful to summarize low energy physics up to about one GeV with an effective chiral Lagrangian. (Evidently the pseudoscalar and vector nonet fields are the raw materials.) The achievement of such a goal seems to require continuous improvement of theory (i.e., the addition of more symmetry breaking terms) as well as the precision of the experimental results. Here we have considered more physical processes to fit than previous treatments and given a more complete enumeration of symmetry breaking terms. All parameters were determined directly from the experimental data and a serious attempt to improve the accuracy of the analysis was made.

Naturally the treatment of symmetry breaking in the system of pseudoscalars plus vectors is considerably more complicated than the already complicated treatment of pseudoscalars alone. In the latter case we have reviewed the fact that, except for terms needed^{‡‡} to solve the U(1) problem, the chiral perturbation theory analysis[1, 2] of chiral symmetry breaking is essentially reproduced at tree level with three OZI rule conserving terms of type \mathcal{M} , $\mathcal{M}\partial^2$ and \mathcal{M}^2 . In practice it seems extremely difficult to definitely establish the existence of non-negligible loop corrections at the level of the one and two point functions involved in the analysis of symmetry breaking (One must go to $\pi\pi$ scattering for this purpose). Such a situation might be expected if the $1/N_c$ approximation is quite good. We have given an analogous treatment of the pseudoscalar plus vector system, including only tree diagrams but allowing higher order symmetry breaking terms which may mask any loop effects. We did, however, give some discussion and speculation on how to provide a controllable expansion scheme in this more complicated situation. We also showed (section 4.1) how the prediction for the decay $\rho^0 \rightarrow e^+e^-$ could be significantly improved either with higher derivative terms or by an old calculation[14] which amounts to the partial inclusion of the loop effects. It would be interesting to further investigate this and related processes in the future.

An interesting question is whether the symmetry breaking patterns (modulo the important but understood difference in the strengths of OZI violation) for the vectors and pseudoscalars are precisely analogous. In other words, do we really need to include “second order” symmetry breaker for the vector nonet? Here we have seen indications that they are needed. Apart from the explanation of the $\rho^0 \rightarrow e^+e^-$ rate mentioned above, the $\mathcal{M}\partial^2$ type γ' term in eq. (2.14) was seen to be helpful for improving the predicted K^0 “charge

^{‡‡} These terms are discussed in ref. [7].

radius". The jury is still out on the need for \mathcal{M}^2 type vector symmetry breakers. We saw that they could increase the size of the $K^{*0}-K^{*+}$ mass difference Δm_{K^*} by a small amount. This would move the prediction in the direction towards the central experimental values. As discussed in detail in section 3.3 it is possible that experiment and theory are already in agreement for Δm_{K^*} but further theoretical analysis of the electromagnetic contribution and a more refined experimental analysis seems necessary.

It should be remarked that the symmetry breaking terms (even though slightly numerous) do not *drastically* change the simple picture, present in the model without symmetry breaking, of vector meson dominance and the associated empirical KSRF formula. Rather they provide "fine tuning". There are just a few *essential* parameters needed to obtain an approximate fit. Furthermore, for the fit presented here, rather conventional values (see eqs. (3.11) and (3.12)) of the quark mass ratios were extracted. The quark mass ratio determination is only subject to the uncertainty of the " Δm_{K^*} puzzle" (sections 3.3 and 3.4). It is interesting to notice that, for the small vector nonet OZI rule violation piece of the Lagrangian, both SU(3) symmetry breaking as well as SU(3) symmetric terms are required. There does not seem to be a multiplicative suppression of OZI violating \times SU(3) violating terms.

We have not presented in this paper an analysis of symmetry breaking effects for the terms of the Lagrangian proportional to the Levi-Civita symbol. This topic will be discussed elsewhere.

Acknowledgements

We would like to thank Francesco Sannino, Anand Subbaraman and Herbert Weigel for helpful discussions. This work was supported in part by the U.S. DOE Contract No. DE-FG-02-85ER40231. One of us (M.H.) acknowledges partial support by the Japan Society for the Promotion of Science.

A Formulae

In this appendix, we list the quantities discussed in this paper computed from our Lagrangian: $\mathcal{L} = \mathcal{L}_{\text{sym}} + \mathcal{L}_{\text{SB}} + \mathcal{L}_{\nu 1} + \mathcal{L}_{\nu 2}$. In the appropriate limits the formulae reduce to those given in ref. [7]; one should replace: $\alpha_+ \rightarrow \alpha'$, $\alpha_- \rightarrow \alpha'$ and $\alpha_p \rightarrow \alpha' - 4\beta'\tilde{g}^2$.

A.1 Alternate form of Lagrangian

Here for comparison with other papers we rewrite our Lagrangian by using the following fields:

$$\begin{aligned} p_\mu &\equiv \frac{i}{2} (\xi \partial_\mu \xi^\dagger - \xi^\dagger \partial_\mu \xi) , \\ v_\mu &\equiv \frac{i}{2} (\xi \partial_\mu \xi^\dagger + \xi^\dagger \partial_\mu \xi) . \end{aligned} \quad (\text{A.1})$$

For the symmetry breaking spurion, the following combinations are convenient:

$$\widehat{\mathcal{M}}_\pm \equiv \frac{1}{2} (\xi \mathcal{M}^\dagger \xi \pm \xi^\dagger \mathcal{M} \xi^\dagger) . \quad (\text{A.2})$$

Using the quantities v_μ and p_μ , the symmetric Lagrangian (2.4) is rewritten as

$$\mathcal{L}_{\text{sym}} = -\frac{1}{2} m_v^2 \text{Tr} [\widehat{\rho}_\mu \widehat{\rho}_\mu] - \frac{F_\pi^2}{2} \text{Tr} [p_\mu p_\mu] - \frac{1}{4} \text{Tr} [F_{\mu\nu}(\rho) F_{\mu\nu}(\rho)] , \quad (\text{A.3})$$

where $\widehat{\rho}_\mu \equiv \rho_\mu - v_\mu/\tilde{g}$. The α_i terms in the first order symmetry breaking terms are rewritten as

$$\mathcal{L}_{\alpha_i} = 2\alpha_+ \text{Tr} [\widehat{\mathcal{M}}_+ \widehat{\rho}_\mu \widehat{\rho}_\mu] - 2\frac{\alpha_-}{\tilde{g}} \text{Tr} [\widehat{\mathcal{M}}_- [\widehat{\rho}_\mu, p_\mu]] - 2\frac{\alpha_p}{\tilde{g}^2} \text{Tr} [\widehat{\mathcal{M}}_+ p_\mu p_\mu] , \quad (\text{A.4})$$

where α_+ , α_- and α_p are defined in table 1. The μ terms in eq. (2.15) are rewritten as

$$\begin{aligned} \mathcal{L}_\mu &= \mu_a \text{Tr} [\widehat{\rho}_\mu \widehat{\mathcal{M}}_+ \widehat{\rho}_\mu \widehat{\mathcal{M}}_+] - \mu_b \text{Tr} [\widehat{\rho}_\mu \widehat{\mathcal{M}}_- \widehat{\rho}_\mu \widehat{\mathcal{M}}_-] - \frac{\mu_c}{\tilde{g}^2} \text{Tr} [p_\mu \widehat{\mathcal{M}}_+ p_\mu \widehat{\mathcal{M}}_+] \\ &\quad + \frac{\mu_d}{\tilde{g}^2} \text{Tr} [p_\mu \widehat{\mathcal{M}}_- p_\mu \widehat{\mathcal{M}}_-] - \frac{2\mu_e}{\tilde{g}} \text{Tr} [\widehat{\rho}_\mu \widehat{\mathcal{M}}_+ p_\mu \widehat{\mathcal{M}}_- - \widehat{\rho}_\mu \widehat{\mathcal{M}}_- p_\mu \widehat{\mathcal{M}}_+] , \end{aligned} \quad (\text{A.5})$$

where μ_a , μ_b , μ_c , μ_d and μ_e are defined in table 1. The OZI rule violating terms in eqs. (2.16) and (2.17) are also rewritten as

$$\mathcal{L}_\nu = \nu_a (\text{Tr} [\widehat{\rho}_\mu])^2 + \nu_b \text{Tr} [\widehat{\rho}_\mu] \text{Tr} [\widehat{\mathcal{M}}_+ \widehat{\rho}_\mu] + \frac{\nu_c}{\tilde{g}^2} (\text{Tr} [p_\mu])^2 + \frac{\nu_d}{\tilde{g}^2} \text{Tr} [p_\mu] \text{Tr} [\widehat{\mathcal{M}}_+ p_\mu] , \quad (\text{A.6})$$

where ν_a , ν_b , ν_c and ν_d are defined in table 1. Note that only the ν_a and ν_b terms are relevant for the vector nonet.

A.2 kinetic terms

The wave function renormalization constants for pseudoscalar and vector mesons defined in eq. (3.2) are given by

$$Z_\pi = \left[1 + \frac{2(2\alpha_p + \mu_c)}{\tilde{g}^2 F_\pi^2} \right]^{1/2}, \quad Z_K = \left[1 + \frac{2(1+x)\alpha_p + 2x\mu_c}{\tilde{g}^2 F_\pi^2} \right]^{1/2}. \quad (\text{A.7})$$

and

$$Z_\rho = Z_\omega = [1 - 8\gamma']^{1/2}, \quad Z_\phi = [1 - 8x\gamma']^{1/2}, \quad Z_{K^*} = [1 - 4\gamma'(1+x)]^{1/2}. \quad (\text{A.8})$$

A.3 masses and mixings

The vector meson masses are given by

$$\begin{aligned} m_\rho^2 &= [m_v^2 - 4\alpha_+ - 2\mu_a] / Z_\rho^2, \\ m_\omega^2 &= [m_v^2 - 4\alpha_+ - 2\mu_a - 4(\nu_a + \nu_b)] / Z_\omega^2, \\ m_\phi^2 &= [m_v^2 - 4x\alpha_+ - 2x^2\mu_a - 2(\nu_a + x\nu_b)] / Z_\phi^2, \\ m_{K^*}^2 &= [m_v^2 - 2(1+x)\alpha_+ - 2x\mu_a] / Z_{K^*}^2. \end{aligned} \quad (\text{A.9})$$

The non-electromagnetic $K^0 - K^+$ and $K^{0*} - K^{+*}$ mass differences are given by

$$\begin{aligned} [\Delta m_K]_{\text{nonEM}} &\equiv [m_{K^0} - m_{K^+}]_{\text{nonEM}} \\ &= \frac{y}{F_{Kp}^2 m_K} \left[-4\delta' - 16(1+x)\lambda'^2 + 2m_K^2 \frac{\alpha_p + x\mu_c}{\tilde{g}^2} \right]. \end{aligned} \quad (\text{A.10})$$

$$[\Delta m_{K^*}]_{\text{nonEM}} \equiv [m_{K^*}^{0*} - m_{K^*}^{+*}]_{\text{nonEM}} = y \left[2\alpha_+ - 4\gamma' m_{K^*}^2 + 2x\mu_a \right] / (m_{K^*} Z_{K^*}^2) \quad (\text{A.11})$$

The $\rho^0 - \omega$ transition mass $M_{\rho\omega}$ is defined in terms of the effective term in the Lagrangian: $-2m_\rho M_{\rho\omega} \rho_\mu^0 \omega_\mu$. This is given by

$$[M_{\rho\omega}]_{\text{nonEM}} = -y \left[2\alpha_+ - 4\gamma' m_\rho^2 + 2\mu_a + \nu_b \right] / (m_\rho Z_\rho^2). \quad (\text{A.12})$$

Similarly, $\phi - \omega$ and $\phi - \rho$ mixings, which are defined by $\mathcal{L} = -\Pi_{\phi\omega} \phi_\mu \omega_\mu$ and $\mathcal{L} = -\Pi_{\phi\rho} \phi_\mu \rho_\mu$, are given by

$$\Pi_{\phi\omega} = \frac{-\sqrt{2}(2\nu_a + (1+x)\nu_b)}{Z_\omega Z_\phi}, \quad (\text{A.13})$$

$$\Pi_{\phi\rho} = \frac{-\sqrt{2}y\nu_b}{Z_\rho Z_\phi}. \quad (\text{A.14})$$

A.4 Vector-Pseudoscalar couplings

We define the VPP' coupling constant $g_{VPP'}$ by

$$\mathcal{L} = -\frac{i}{\sqrt{2}}g_{VPP'}V_\mu(\partial_\mu PP' - \partial_\mu P'P) . \quad (\text{A.15})$$

We list the forms of these couplings:

$$\begin{aligned} g_{\rho^0\pi^+\pi^-} &= \left[m_v^2 - 4\alpha_+ + 8\alpha_- - 2\mu_a - 8\mu_e\right]/(\tilde{g}F_{\pi p}^2Z_\rho) , \\ g_{\rho^0K^+K^-} &= \frac{1}{2}\left[m_v^2 - 4\alpha_+ + 4(1+x)\alpha_- - 2\mu_a - 4(1+x)\mu_e\right]/(\tilde{g}F_{Kp}^2Z_\rho) , \\ g_{\rho^0K^0\bar{K}^0} &= -g'_{\rho^0K^+K^-} , \\ g_{\omega K^+K^-} &= \frac{1}{2}\left[m_v^2 - 4\alpha_+ + 4(1+x)\alpha_- - 2\mu_a - 4(1+x)\mu_e + 2(x-1)\nu_b\right]/(\tilde{g}F_{Kp}^2Z_\rho) , \\ g_{\omega K^0\bar{K}^0} &= g_{\omega K^+K^-} , \\ g_{\phi K^+K^-} &= -\frac{1}{\sqrt{2}}\left[m_v^2 - 4x\alpha_+ + 4(1+x)\alpha_- - 2x^2\mu_a - 4x(1+x)\mu_e - (x-1)\nu_b\right]/(\tilde{g}F_{Kp}^2Z_\phi) , \\ g_{\phi K^0\bar{K}^0} &= g_{\phi K^+K^-} , \\ g_{K^{*+}K^-\pi^0} &= \frac{1}{2}\left[m_v^2 - 2(1+x)\alpha_+ + 2(x+3)\alpha_- - 2x\mu_a - 2(3x+1)\mu_e\right]/(\tilde{g}F_{Kp}F_{\pi p}Z_{K^*}) , \\ g_{K^{*+}\bar{K}^0\pi^-} &= g_{K^{*0}K^-\pi^+} = \sqrt{2}g_{K^{*+}K^-\pi^0} , \\ g_{K^{*0}\bar{K}^0\pi^0} &= g_{K^{*+}K^-\pi^0} . \end{aligned} \quad (\text{A.16})$$

Here for later convenience we define the following VPP' couplings $g_{VPP'}$

$$g_{\phi K\bar{K}} = -\sqrt{2}g_{\phi K^+K^-} , \quad g_{K^*K\pi} = 2g_{K^{*+}K^-\pi^0} . \quad (\text{A.17})$$

The isospin breaking vertices are given by

$$g_{\omega\pi\pi} = -2y\left[2\alpha_+ + 2\mu_a + 4\mu_e + \nu_b\right]/(\tilde{g}F_{\pi p}^2Z_\omega) , \quad (\text{A.18})$$

$$g_{\phi\pi^+\pi^-} = -y\frac{\sqrt{2}\nu_b}{\tilde{g}F_{\pi p}^2Z_\phi} . \quad (\text{A.19})$$

A.5 $V-\gamma$ transition terms

The expressions for the vector meson-photon transition strengths defined in eq. (4.1) are given by

$$g_\rho = \frac{1}{Z_\rho}\frac{m_v^2 - 4\alpha_+ - 2\mu_a}{\sqrt{2}\tilde{g}} = \frac{m_\rho^2 Z_\rho}{\sqrt{2}\tilde{g}} ,$$

$$\begin{aligned}
g_\omega &= \frac{1}{3} \frac{1}{Z_\omega} \frac{m_v^2 - 4\alpha_+ - 2\mu_a + 2(x-1)\nu_b}{\sqrt{2}\tilde{g}} = \frac{1}{3} \frac{m_\omega^2 Z_\rho}{\sqrt{2}\tilde{g}} \left[1 - \frac{Z_\phi}{Z_\rho} \frac{\sqrt{2}\Pi_{\phi\omega}}{m_\omega^2} \right] , \\
g_\phi &= -\frac{\sqrt{2}}{3} \frac{1}{Z_\phi} \frac{m_v^2 - 4x\alpha_+ - 2x^2\mu_a - (x-1)\nu_b}{\sqrt{2}\tilde{g}} = -\frac{\sqrt{2}}{3} \frac{m_\phi^2 Z_\phi}{\sqrt{2}\tilde{g}} \left[1 - \frac{Z_\rho}{Z_\phi} \frac{\sqrt{2}\Pi_{\phi\omega}}{2m_\phi^2} \right] . \quad (\text{A.20})
\end{aligned}$$

B Details of $\phi \rightarrow \pi\gamma$ calculation

This process is important for estimating the strength of the ϕ_μ - ω_μ mixing coefficient $\Pi_{\phi\omega}$. As a potentially non-negligible correction we also compute the π^0 - η mixing mediated contribution shown in fig. 1(b). In ref. [31] the ϕ - ω mixing was considered to be the only source for this decay.

B.1 π^0 - η mixing

First we describe the π^0 - η mixing. It is convenient to define $\eta_T \equiv (\phi_{11} + \phi_{22})/\sqrt{2}$ and $\eta_S \equiv \phi_{33}$. Following ref. [7], let us write the relation between these fields and the physical η and η' fields as

$$\begin{aligned} \begin{pmatrix} \eta_T \\ \eta_S \end{pmatrix} &= \begin{pmatrix} A_{11} & A_{12} \\ A_{21} & A_{22} \end{pmatrix} \begin{pmatrix} \eta \\ \eta' \end{pmatrix} , \\ \begin{pmatrix} A_{11} & A_{12} \\ A_{21} & A_{22} \end{pmatrix} &= \begin{pmatrix} \cos \theta_1 & \sin \theta_1 \\ -\sin \theta_1 & \cos \theta_1 \end{pmatrix} \begin{pmatrix} \widehat{K}_1^{-1/2} & 0 \\ 0 & \widehat{K}_2^{-1/2} \end{pmatrix} \begin{pmatrix} \cos \theta_2 & \sin \theta_2 \\ -\sin \theta_2 & \cos \theta_2 \end{pmatrix} . \end{aligned} \quad (\text{B.1})$$

In this paper we shall use the values for these parameters shown in ref. [7]:

$$\theta_1 = 7.44^\circ, \quad \theta_2 = 34.7^\circ, \quad \widehat{K}_1^{1/2} = 1.07, \quad \widehat{K}_2^{1/2} = 1.36 . \quad (\text{B.2})$$

In the present model, there are both mass type and kinetic type π^0 - η_T mixings. These are given by

$$\mathcal{L} = -K_{\pi\eta}\partial_\mu\pi^0\partial_\mu\eta_T - \Pi_{\pi\eta}\pi^0\eta_T , \quad (\text{B.3})$$

where

$$K_{\pi\eta} = 4y \frac{\alpha_p}{\tilde{g}^2 F_\pi F_{\pi p}} , \quad \Pi_{\pi\eta} = \frac{8y}{F_\pi F_{\pi p}} [\delta' + 8\lambda'^2] . \quad (\text{B.4})$$

After diagonalizing the η - η' part as shown in eq. (B.1), we include the π^0 - η mixing effect by introducing the following physical fields:

$$\begin{pmatrix} \pi^0 \\ \eta \end{pmatrix} = \begin{pmatrix} 1 & \varepsilon_{12} \\ \varepsilon_{21} & 1 \end{pmatrix} \begin{pmatrix} \pi_p^0 \\ \eta_p \end{pmatrix} , \quad (\text{B.5})$$

where

$$\varepsilon_{12} = A_{11} \frac{\Pi_{\pi\eta} - K_{\pi\eta} m_\eta^2}{m_\eta^2 - m_\pi^2} , \quad \varepsilon_{21} = -A_{11} \frac{\Pi_{\pi\eta} - K_{\pi\eta} m_\pi^2}{m_\eta^2 - m_\pi^2} . \quad (\text{B.6})$$

B.2 $\phi \rightarrow \pi\gamma$ decay

The partial width of the $V \rightarrow P\gamma$ decay process (V : vector meson, P : pseudoscalar meson) is given by

$$\Gamma(V \rightarrow P\gamma) = \frac{3\alpha|q_\gamma(V)|^3}{32\pi^4 F_{\pi p}^2} |G_{VP\gamma}|^2 , \quad (\text{B.7})$$

where $q_\gamma(V) = (m_V^2 - m_P^2)/(2m_V)$ and $G_{VP\gamma}$ is defined by

$$\mathcal{L} = \frac{3e}{4\sqrt{2}\pi^2 F_{\pi p}} G_{VP\gamma} \varepsilon_{\mu\nu\lambda\sigma} \partial_\mu V_\nu \partial_\lambda \mathcal{A}_\sigma P . \quad (\text{B.8})$$

Using the experimental values $\Gamma(\omega \rightarrow \pi^0\gamma) = 0.72(\text{MeV})$ and $\Gamma(\phi \rightarrow \eta\gamma) = 5.8(\text{GeV})$, we find $|G_{\omega\pi\gamma}| = 5.7$, $|G_{\phi\eta\gamma}| = 1.7$. If we consider that ϕ – ω mixing and π – η mixing are the sources for $\phi \rightarrow \pi^0\gamma$ decay, the effective coupling for this decay is related to these two couplings as

$$G_{\phi\pi\gamma} = \frac{\Pi_{\phi\omega}}{m_\phi^2 - m_\omega^2} G_{\omega\pi\gamma} + \varepsilon_{21} G_{\phi\eta\gamma} , \quad (\text{B.9})$$

where $\Pi_{\phi\omega}$ is given in eq. (A.13) while ε_{21} is given in eq. (B.6).

To determine the value of $G_{\phi\pi\gamma}$ we need to know the relative sign between $G_{\omega\pi\gamma}$ and $G_{\phi\eta\gamma}$. As shown, for example, in refs. [32, 31] both terms are part of a single trace and one obtains $R_{\phi\omega} \equiv G_{\phi\eta\gamma}/G_{\omega\pi\gamma} = -2A_{21}/3$, where A_{21} is a component of the η – η' mixing matrix. Using the values in eqs. (B.2) we find $A_{21} = -0.52$, and $R_{\phi\omega} = 0.35$ which agrees with the experiment (Experimentally $|R_{\phi\omega}| = 0.30$). Then we can take both $G_{\omega\pi\gamma}$ and $G_{\phi\eta\gamma}$ to be positive for present purposes and set

$$G_{\omega\pi\gamma} = 5.7 , \quad G_{\phi\eta\gamma} = 1.7 , \quad A_{11} = 0.71 , \quad (\text{B.10})$$

where for A_{11} we use the values in eqs. (B.2).

C $\omega \rightarrow \pi^+ \pi^-$ and $\phi \rightarrow \pi^+ \pi^-$ decay processes

There are two main contributions to the isospin breaking decay $\omega \rightarrow \pi^+ \pi^-$: (1) ρ - ω mixing $M_{\rho\omega}$; (2) the isospin breaking direct $\omega \pi^+ \pi^-$ vertex $g_{\omega\pi\pi}$. As discussed in ref. [13], the masses of the ρ and ω mesons are so close that it is important to take the widths into account for the effect of ρ - ω mixing. Then the ratio of $\pi\pi$ decay width of ω to that of ρ is given by

$$\frac{\Gamma(\omega \rightarrow \pi^+ \pi^-)}{\Gamma(\rho \rightarrow \pi^+ \pi^-)} = \left| \frac{g_{\omega\pi\pi}}{g_{\rho\pi\pi}} + \frac{M_{\rho\omega}}{m_\omega - m_\rho - \frac{i}{2}(\Gamma_\omega - \Gamma_\rho)} \right|^2 \left| \frac{q_\pi(\omega)}{q_\pi(\rho)} \right|^3 \frac{m_\rho^2}{m_\omega^2}, \quad (\text{C.1})$$

where $q_\pi(V) \equiv \frac{1}{2}\sqrt{m_V^2 - 4m_\pi^2}$, ($V = \rho, \omega$). The experimental value of this ratio is estimated as $(1.23 \pm 0.19) \times 10^{-3}$. For the experimental fit of this process it is important to include the electromagnetic contribution to the ρ - ω mixing. This is estimated as [13]

$$[M_{\rho\omega}]_{\text{EM}} = \frac{3}{2\alpha} \sqrt{\frac{m_\omega}{m_\rho}} \sqrt{\Gamma(\rho \rightarrow e^+ e^-) \Gamma(\omega \rightarrow e^+ e^-)} \simeq (0.417 \pm 0.017) \text{ MeV}. \quad (\text{C.2})$$

For comparison, we consider the case where the direct $\omega \pi\pi$ vertex is negligible ($g_{\omega\pi\pi} \simeq 0$). Using the above formula (C.1) with $g_{\omega\pi\pi} = 0$, we obtain

$$M_{\rho\omega} = -(2.50 \pm 0.20) \text{ MeV}, \quad [M_{\rho\omega}]_{\text{nonEM}} = -(2.92 \pm 0.22) \text{ MeV}. \quad (\text{C.3})$$

Similarly, for the $\phi \rightarrow \pi^+ \pi^-$ process, the main contribution is given by the $\phi\rho$ mixing $\Pi_{\phi\rho}$ and there is a relatively small direct $\phi\pi\pi$ coupling $g_{\phi\pi\pi}$. We then have

$$\frac{\Gamma(\phi \rightarrow \pi^+ \pi^-)}{\Gamma(\rho \rightarrow \pi^+ \pi^-)} = \left| \frac{g_{\phi\pi\pi}}{g_{\rho\pi\pi}} + \frac{\Pi_{\phi\rho}}{m_\phi^2 - m_\rho^2} \right|^2 \left| \frac{\mathbf{q}_\pi(\phi)}{\mathbf{q}_\pi(\rho)} \right|^3 \frac{m_\rho^2}{m_\phi^2}. \quad (\text{C.4})$$

Experimentally, this ratio is estimated as $(2.3^{+1.5}_{-1.2}) \times 10^{-6}$. The electromagnetic contribution to the ϕ - ω mixing is estimated as

$$[\Pi_{\phi\omega}]_{\text{EM}} = \frac{3}{\alpha} m_\omega \frac{m_\omega}{m_\phi} \sqrt{\Gamma(\phi \rightarrow e^+ e^-) \Gamma(\omega \rightarrow e^+ e^-)} \simeq (0.255 \pm 0.006) \times 10^{-3} (\text{GeV}^2). \quad (\text{C.5})$$

This is very small compared with the nonelectromagnetic contribution, and we neglect it in this paper.

References

- [1] S. Weinberg, *Physica* **96A**, 327 (1979).
- [2] J. Gasser and H. Leutwyler, *Ann. Phys. (N.Y.)* **158**, 142 (1984); *Nucl. Phys.* **B250**, 465 (1985).
- [3] J. Cronin, *Phys. Rev.* **161**, 1483 (1967).
- [4] J. Donoghue, C. Ramirez, and G. Valencia, *Phys. Rev. D* **39**, 1947 (1989);
G. Ecker, J. Gasser, A. Pich, and E. de Rafael, *Nucl. Phys.* **B321**, 311 (1989);
G. Ecker and J. Gasser and H. Leutwyler and A. Pich and E. de Rafael, *Phys. Lett. B* **233**, 425 (1989).
- [5] G. 'tHooft, *Nucl. Phys.* **B75**, 461 (1974);
E. Witten, *Nucl. Phys.* **B149**, 285 (1979).
- [6] F. Sannino and J. Schechter, Syracuse University Report **No. SU-4240-601**, 1995 (unpublished).
- [7] J. Schechter, A. Subbaraman, and H. Weigel, *Phys. Rev. D* **48**, 339 (1993).
- [8] M. Bando, T. Kugo and K. Yamawaki, *Nucl. Phys.* **B259**, 493 (1985).
- [9] A. Bramon, A. Grau, and G. Pancheri, *Phys. Lett. B* **345**, 263 (1995).
- [10] S. Furui, R. Kobayashi, and M. Nakagawa, Meijo University Report **No. MJU-DP-501/ISM-181**, 1995 (unpublished).
- [11] S. Okubo, *Phys. Lett.* **5**, 165 (1963);
G. Zweig, CERN Reports **No. 8182/TH 401, 8419/TH 412**, 1964 (unpublished);
J. Iizuka, *Prog. Theor. Phys. Suppl.* **37-8**, 21 (1966).
- [12] R. Dashen, *Phys. Rev.* **183**, 1245 (1969).
- [13] J. Gasser and H. Leutwyler, *Phys. Rep.* **87**, 77 (1982).
- [14] G. Gounaris and J. Sakurai, *Phys. Rev. Lett.* **21**, 244 (1968).
- [15] Ö. Kaymakcalan and J. Schechter, *Phys. Rev. D* **31**, 1109 (1985).

- [16] M. Bando, T. Kugo and K. Yamawaki, Phys. Rep. **164**, 217 (1988).
- [17] K. Kawarabayashi and M. Suzuki, Phys. Rev. Lett. **16**, 255 (1966);
Riazuddin and Fayyazuddin, Phys. Rev. **147**, 1071 (1966).
- [18] J. Schechter, Phys. Rev. D **34**, 868 (1986).
- [19] Particle Data Group, Phys. Rev. D **50**, 1173 (1994).
- [20] N.G. Deshpande, D.A. Dicus, K. Johnson and V. Teplitz, Phys. Rev. D **15**, 1885 (1977).
- [21] H.B. O'Connell, B.C. Pearce, A.W. Thomas and A. Williams, Adelaide University Report **No. ADP-95-15/T176**, 1995 (unpublished).
- [22] W.R. Molzon et al., Phys. Rev. Lett. **41**, 1213 (1978).
- [23] E.B. Dally et al., Phys. Rev. Lett. **39**, 1176 (1977).
- [24] E.B. Dally et al., Phys. Rev. Lett. **45**, 232 (1980).
- [25] E.B. Dally et al., Phys. Rev. Lett. **48**, 375 (1982).
- [26] S.R. Amendolia et al., Phys. Lett. **146B**, 116 (1984).
- [27] L.M. Barkov et al., Nucl. Phys. **B256**, 365 (1985).
- [28] S.R. Amendolia et al., Phys. Lett. B **178**, 435 (1986).
- [29] S.R. Amendolia et al., Nucl. Phys. **B277**, 168 (1986).
- [30] C. Erkal and M. Olsson, J. Phys. G **13**, 1355 (1987).
- [31] P. Jain, R. Johnson, Ulf-G. Meissner, N. W. Park and J. Schechter, Phys. Rev. D **37**, 3252 (1988).
- [32] T. Fujiwara, T. Kugo, H. Terao, S. Uehara and K. Yamawaki, Prog. Theor. Phys. **73**, 926 (1985).